Measurement of the W boson polarisation in $t\bar{t}$ events from pp collisions at $\sqrt{s}$ = 8 TeV in the lepton + jets channel with ATLAS

Measurement of the *W* boson polarisation in $t\bar{t}$ events from *pp* collisions at $\sqrt{s}$ = 8 TeV in the lepton + jets channel with ATLAS

ATLAS Collaboration*

CERN, 1211 Geneva 23, Switzerland

Abstract This paper presents a measurement of the polarisation of *W* bosons from $t\bar{t}$ decays, reconstructed in events with one high-p_T lepton and at least four jets. Data from *pp* collisions at the LHC were collected at $\sqrt{s}$ = 8 TeV and correspond to an integrated luminosity of 20.2 fb^{-1}. The angle θ^* between the *b*-quark from the top quark decay and a direct *W* boson decay product in the *W* boson rest frame is sensitive to the *W* boson polarisation. Two different *W* decay products are used as polarisation analysers: the charged lepton and the down-type quark for the leptonically and hadronically decaying *W* boson, respectively. The most precise measurement of the *W* boson polarisation via the distribution of $\cos\theta^*$ is obtained using the leptonic analyser and events in which at least two of the jets are tagged as *b*-quark jets. The fitted fractions of longitudinal, left- and right-handed polarisation states are $F_0 = 0.709 \pm 0.019$, $F_L = 0.299 \pm 0.015$ and $F_R = -0.008 \pm 0.014$, and are the most precisely measured *W* boson polarisation fractions to date. Limits on anomalous couplings of the Wtb vertex are set.

1 Introduction

The top quark, discovered in 1995 by the CDF and D0 collaborations [1,2] is the heaviest known elementary particle. It decays almost exclusively into a *W* boson and a *b*-quark. The properties of the top decay vertex Wtb are determined by the structure of the weak interaction. In the Standard Model (SM) this interaction has a $(V - A)$ structure, where *V* and *A* refer to the vector and axial vector components of the weak coupling. The *W* boson, which is produced as a real particle in the decay of top quarks, possesses a polarisation which can be left-handed, right-handed or longitudinal. The corresponding fractions, referred to as helicity fractions, are determined by the Wtb vertex structure and the masses of the particles involved. Calculations at next-to-next-to-leading order (NNLO) in QCD predict the frac-

tions to be $F_L = 0.311 \pm 0.005$, $F_R = 0.0017 \pm 0.0001$, $F_0 = 0.687 \pm 0.005$ [3].

By measuring the polarisation of the *W* boson with high precision, the SM prediction can be tested, and new physics processes which modify the structure of the Wtb vertex can be probed. The structure of the Wtb vertex can be expressed in a general form using left- and right-handed vector ($V_{L/R}$) and tensor ($g_{L/R}$) couplings:

$$\mathcal{L}_{Wtb} = -\frac{g}{\sqrt{2}} \bar{b} \gamma^\mu (V_L P_L + V_R P_R) t\, W_\mu^-$$
$$-\frac{g}{\sqrt{2}} \bar{b} \frac{i\sigma^{\mu\nu} q_\nu}{m_W} (g_L P_L + g_R P_R) t\, W_\mu^- + \text{h.c.} \quad (1)$$

Here, $P_{L/R}$ refer to the left- and right-handed chirality projection operators, m_W to the *W* boson mass, and *g* to the weak coupling constant. At tree level, all of the vector and tensor couplings vanish in the SM, except V_L, which corresponds to the CKM matrix element V_{tb} and has a value of approximately one. Dimension-six operators, introduced in effective field theories, can lead to anomalous couplings, represented by non-vanishing values of V_R, g_L and g_R [4–6].

The *W* boson helicity fractions can be accessed via angular distributions of polarisation analysers. Such analysers are *W* boson decay products whose angular distribution is sensitive to the *W* polarisation and determined by the Wtb vertex structure. In case of a leptonic decay of the *W* boson ($W \to \ell\nu$), the charged lepton serves as an ideal analyser: its reconstruction efficiency is very high and the sensitivity of its angular distribution to the *W* boson polarisation is maximal due to its weak isospin component $T_3 = -\frac{1}{2}$. If the *W* boson decays hadronically ($W \to q\bar{q}'$), the down-type quark is used, as it carries the same weak isospin as the charged lepton. This provides it with the same analysing power as the charged lepton, which is only degraded by the lower reconstruction efficiency and resolution of jets compared to charged leptons. The reconstruction of the down-type quark is in particular difficult as the two decay products of a hadronically decaying *W* boson are experimentally hard

Springer

to separate. In the W boson rest frame, the differential cross-section of the analyser follows the distribution

$$\frac{1}{\sigma}\frac{\mathrm{d}\sigma}{\mathrm{d}\cos\theta^*} = \frac{3}{4}\left(1-\cos^2\theta^*\right) F_0$$
$$+\frac{3}{8}\left(1-\cos\theta^*\right)^2 F_{\mathrm{L}} + \frac{3}{8}\left(1+\cos\theta^*\right)^2 F_{\mathrm{R}}, \tag{2}$$

which directly relates the W boson helicity fractions F_i to the angle θ^* between the analyser and the reversed direction of flight of the b-quark from the top quark decay in the W boson rest frame. Previous measurements of the W boson helicity fractions from the ATLAS, CDF, CMS and D0 collaborations show agreement with the SM within the uncertainties [7–11].

In this paper, the W boson helicity fractions are measured in top quark pair ($t\bar{t}$) events. Data corresponding to an integrated luminosity of 20.2 fb^{-1} of proton–proton (pp) collisions, produced at the LHC with a centre-of-mass energy of $\sqrt{s} = 8$ TeV, and recorded with the ATLAS [12] detector, are analysed. The final state of the $t\bar{t}$ events is characterised by the decay of the W bosons. This analysis considers the lepton+jets channel in which one of the W bosons decays leptonically and the other decays hadronically. Both W boson decay modes are utilised for the measurement of $\cos\theta^*$. The signal selection and reconstruction includes direct decays of the W boson into an electron or muon as well as W boson decays into a τ-lepton which subsequently decays leptonically.

2 The ATLAS detector

The ATLAS experiment at the LHC is a multi-purpose particle detector with a forward-backward symmetric cylindrical geometry and a near 4π coverage in solid angle.[1] It consists of an inner tracking detector surrounded by a thin superconducting solenoid providing a 2 T axial magnetic field, electromagnetic and hadron calorimeters, and a muon spectrometer. The inner tracking detector covers the pseudorapidity range $|\eta| < 2.5$. It consists of silicon pixel, silicon microstrip, and transition-radiation tracking detectors. Lead/liquid-argon (LAr) sampling calorimeters provide electromagnetic energy measurements with high granularity. A hadron (steel/scintillator-tile) calorimeter covers the central pseudorapidity range ($|\eta| < 1.7$). The end-cap and forward

regions are instrumented with LAr calorimeters for electromagnetic and hadronic energy measurements up to $|\eta| = 4.9$. The muon spectrometer surrounds the calorimeters and is based on three large air-core toroid superconducting magnets with eight coils each. Its bending power ranges from 2.0 to 7.5 T m. It includes a system of precision tracking chambers and fast detectors for triggering. A three-level trigger system is used to select events. The first-level trigger is implemented in hardware and uses a subset of the detector information to reduce the accepted rate to at most 75 kHz. This is followed by the high-level trigger, two software-based trigger levels that together reduce the accepted event rate to 400 Hz on average depending on the data-taking conditions.

3 Data and simulated samples

The data set consists of pp collisions, recorded at the LHC with $\sqrt{s} = 8$ TeV, and corresponds to an integrated luminosity of 20.2 fb^{-1}. Single-lepton triggers with a threshold of 24 GeV of transverse momentum (energy) for isolated muons (electrons) and 36 (60) GeV for muons (electrons) without an isolation criterion are used to select $t\bar{t}$ candidate events. The lower trigger thresholds include isolation requirements on the candidate lepton, resulting in inefficiencies at high p_{T} that are recovered by the triggers with higher p_{T} thresholds.

Samples obtained from Monte Carlo (MC) simulations are used to characterise the detector response and reconstruction efficiency of $t\bar{t}$ events, estimate systematic uncertainties and predict the background contributions from various processes. The response of the full ATLAS detector is simulated [13] using GEANT 4 [14]. For the estimation of some systematic uncertainties, generated samples are passed through a faster simulation with parameterised showers in the calorimeters [15], while still using the full simulation of the tracking systems. Simulated events include the effect of multiple pp collisions from the same and nearby bunch-crossings (in-time and out-of-time pile-up) and are reweighted to match the number of collisions observed in data. All simulated samples are normalised using the most precise cross-section calculations available.

Signal $t\bar{t}$ events are generated using the next-to-leading-order (NLO) QCD MC event generator POWHEG-BOX [16–19] using the CT10 parton distribution function (PDF) set [20]. POWHEG-BOX is interfaced to PYTHIA 6.425 [21] (referred to as the POWHEG+PYTHIA sample), which is used to model the showering and hadronisation, with the CTEQ6L1 PDF set [22] and a set of tuned parameters called the Perugia2011C tune [23] for the modelling of the underlying event. The model parameter h_{damp} is set to m_t and controls matrix element to parton shower matching in POWHEG-BOX and effectively regulates the amount of high-p_{T} radiation.

---

[1] ATLAS uses a right-handed coordinate system with its origin at the nominal interaction point (IP) in the centre of the detector and the z-axis along the beam pipe. The x-axis points from the IP to the centre of the LHC ring, and the y-axis points upwards. Cylindrical coordinates (r, ϕ) are used in the transverse plane, ϕ being the azimuthal angle around the z-axis. The pseudorapidity is defined in terms of the polar angle θ as $\eta = -\ln\tan(\theta/2)$. The angular distance is measured in units of $\Delta R \equiv \sqrt{(\Delta\eta)^2 + (\Delta\phi)^2}$.

The $t\bar{t}$ cross-section is $\sigma(t\bar{t}) = 253^{+13}_{-15}$ pb. This value is the result of a NNLO QCD calculation that includes resummation of next-to-next-to-leading logarithmic soft gluon terms with top++2.0 [24–30].

A sample generated with POWHEG-BOX interfaced with HERWIG 6.520 [31] using Jimmy 4.31 [32] to simulate the underlying event (referred to as the POWHEG+HERWIG sample) is compared to a POWHEG+PYTHIA sample to assess the impact of the different parton shower models. For both the POWHEG+HERWIG sample and this alternate POWHEG+PYTHIA sample, the h_{damp} parameter is set to infinity.

To estimate the uncertainty due to the choice of the MC event generator, an alternate $t\bar{t}$ MC sample is produced with MC@NLO [33,34] with the CT10 PDF set interfaced to HERWIG 6.520 using the AUET2 tune [35] and the CT10 PDF set for showering and hadronisation. In addition, samples generated with POWHEG-BOX interfaced to PYTHIA with variations in the amount of QCD initial- and final-state radiation (ISR/FSR) are used to estimate the effect of such uncertainty. The factorisation and renormalisation scales and the h_{damp} parameter in POWHEG-BOX as well as the transverse momentum scale of the space-like parton-shower evolution in PYTHIA are varied within the constraints obtained from an ATLAS measurement of $t\bar{t}$ production in association with jets [36].

Single-top-quark-processes for the t-channel, s-channel and Wt associated production are also simulated with POWHEG-BOX [37,38] using the CT10 PDF set. The samples are interfaced to PYTHIA 6.425 with the CTEQ6L1 PDF set and the Perugia2011C underlying event tune. Overlaps between the $t\bar{t}$ and Wt final states are removed [39]. The single-top-quark samples are normalised using the approximate NNLO theoretical cross-sections [40–42] calculated with the MSTW2008 NNLO PDF set [43,44]. All $t\bar{t}$ and single-top samples are generated assuming a top quark mass of 172.5 GeV, compatible with the ATLAS measurement of $m_t = 172.84 \pm 0.70$ GeV [45].

Events with a W or Z boson produced in association with jets are generated using the leading-order (LO) event generator ALPGEN 2.14 [46] with up to five additional partons and the CTEQ6L1 PDF set, interfaced to PYTHIA 6.425 for the parton showering and hadronisation. Separate samples for W/Z+light-jets, $W/Zb\bar{b}$+jets, $W/Zc\bar{c}$+jets and Wc+jets were generated. A parton–jet matching scheme ("MLM matching") [47] is employed to avoid double-counting of jets generated from the matrix element and the parton shower. Overlap between the $W/ZQ\bar{Q}$ ($Q = b, c$) events generated at the matrix element level and those generated by the parton shower evolution of the W/Z+light-jets sample are removed with an angular separation algorithm. If the angular distance ΔR between the heavy-quark pair is larger than 0.4, the matrix element prediction is used instead of the par-

ton shower prediction. Event yields from the Z+jets background are normalised using their inclusive NNLO theoretical cross-sections [48]. The predictions of normalisation and flavour composition of the W+jets background are affected by large uncertainties. Hence, a data-driven technique is used to determine both the inclusive normalisation and the heavy-flavour fractions of this process. The approach followed exploits the fact that the $W^{\pm}$ boson production is charge-asymmetric at a pp collider. The W boson charge asymmetry depends on the flavour composition of the sample. Thus, correction factors estimated from data are used to rescale the fractions of $Wb\bar{b}/c\bar{c}$+jets, Wc+jets and W+light-jets events in the MC simulation: $K_{bb} = K_{cc} = 1.50 \pm 0.11$ (stat. + syst.), $K_c = 1.07 \pm 0.27$ (stat. + syst.) and $K_{\mathrm{light}} = 0.80 \pm 0.04$ (stat. + syst.) [49].

Diboson samples (WW, ZZ, WZ) are generated using the SHERPA 1.4.1 [50] event generator with the CT10 PDF set, with massive b- and c-quarks and with up to three additional partons in the LO matrix elements. The yields of these backgrounds are normalised using their NLO QCD theoretical cross-sections [51].

Multijet events can contain jets misidentified as leptons or non-prompt leptons from hadron decays and hence satisfy the selection criteria of the lepton+jets topology. This source of background events is referred to as fake-lepton background and is estimated using a data-driven approach ("matrix method") which is based on the measurement of lepton selection efficiencies using different identification and isolation criteria [52].

4 Event selection and $t\bar{t}$ reconstruction

4.1 Object reconstruction

The final state contains electrons, muons, jets with some of them originating from b-quarks, as well as missing transverse momentum.

Electrons are reconstructed from energy depositions in the electromagnetic calorimeter matching tracks in the inner detector. The transverse component of the energy deposition has to exceed 25 GeV and the pseudorapidity of the energy cluster, η_{cluster}, has to fullfil $|\eta_{\mathrm{cluster}}| < 2.47$, excluding the transition region between the barrel and end-cap sections of the electromagnetic calorimeter at $1.37 < |\eta_{\mathrm{cluster}}| < 1.52$. Electrons are further required to have a longitudinal impact parameter with respect to the hard-scattering vertex of less than 2 mm.

To reduce the background from non-prompt electrons (i.e. electrons produced within jets), electron candidates are also required to be isolated. Two η-dependent isolation criteria are applied. The first one considers the energy deposited in the calorimeter cells within a cone of size $\Delta R = 0.2$ around

the electron direction. The second one sums the transverse momenta (p_T) of all tracks with $p_T > 400$ MeV within a cone of size $\Delta R = 0.3$ around the electron track. For each quantity, the transverse energy or momentum of the electron are subtracted. The isolation requirement is applied in such a way as to retain 90% of signal electrons, independent of their p_T value. This constant efficiency is verified in a data sample of $Z \rightarrow ee$ decays [53].

For the reconstruction of muons, information from the muon spectrometer and the inner detector is combined. The combined muon track must satisfy $p_T > 25$ GeV and $|\eta| < 2.5$. The longitudinal impact parameter with respect to the hard-scattering vertex (defined in next section) is required to be less than 2 mm. Furthermore, muons are required to satisfy a p_T-dependent track-based isolation requirement. The scalar sum of the track p_T in a cone of variable size $\Delta R < 10 \, \text{GeV}/p_T^\mu$ around the muon (excluding the muon track itself) has to be less than 5% of the muon p_T.

Jets are reconstructed from topological clusters [12] built from energy depositions in the calorimeters using the anti-k_t algorithm [54,55] with a radius parameter of 0.4. Before being processed by the jet-finding algorithm, the topological cluster energies are corrected using a local calibration scheme [56,57] to account for inactive detector material, out-of-cluster leakage and the noncompensating calorimeter response. After energy calibration [58], the jets are required to have $p_T > 25$ GeV and $|\eta| < 2.5$. To suppress jets from pile-up, the jet vertex fraction[2] is required to be above 0.5 for all jets with $p_T < 50$ GeV and $|\eta| < 2.4$. As all electron candidates are also reconstructed as jets, the closest jet within a cone of size $\Delta R = 0.2$ around an electron candidate is discarded to avoid double-counting of electrons as jets. After this removal procedure, electrons within $\Delta R = 0.4$ of any remaining jet are removed.

Jets are identified as originating from the hadronisation of a b-quark (b-tagged) via a multivariate algorithm [59]. It makes use of the lifetime and mass of b-hadrons and accounts for displaced tracks and topological properties of the jets. A working point with 70% efficiency to tag a b-quark jet (b-jet) is used. The rejection factor for light-quark and gluon jets (light jets) is around 130 and about 5 for charm jets, as determined for b-tagged jets with $p_T > 20$ GeV and $|\eta| < 2.5$ in simulated $t\bar{t}$ events. The simulated b-tagging efficiency is corrected to that measured in data using calibrations from statistically independent event samples of $t\bar{t}$ pairs decaying into a $b\bar{b}\ell^+\ell^- \nu_\ell \bar{\nu}_\ell$ final state [60].

The reconstruction of the transverse momentum of the neutrino from the leptonically decaying W boson is based on the negative vector sum of all energy deposits and momenta of reconstructed and calibrated objects in the transverse plane (missing transverse momentum with magnitude E_T^{miss}) as well as unassociated energy depositions [61].

4.2 Event selection

Events are selected from data taken in stable beam conditions with all relevant detector components being functional. At least one primary collision vertex is required with at least five associated tracks with $p_T > 400$ MeV. If more than one primary vertex is reconstructed, the one with the largest scalar sum of transverse momenta is selected as the hard-scattering vertex. If the event contains at least one jet with $p_T > 20$ GeV that is identified as out-of-time activity from a previous pp collision or as calorimeter noise [62], the event is rejected.

In order to select events from $t\bar{t}$ decays in the lepton+jets channel, exactly one reconstructed electron or muon with $p_T > 25$ GeV and at least four jets, of which at least one is b-tagged, are required. A match ($\Delta R < 0.15$) between the offline reconstructed electron or muon and the lepton reconstructed by the high-level trigger is required. The selected events are separated into two orthogonal b-tag regions: one region with exactly one b-tag and a second region with two or more b-tags. Thus, the data sample is split into four channels depending on the lepton flavour and the b-jet multiplicity: "e+jets, 1 b-tag", "e+jets, ≥ 2 b-tags", "μ+jets, 1 b-tag" and "μ+jets, ≥ 2 b-tags".

For events with one b-tag, E_T^{miss} is required to be greater than 20 GeV and the sum of E_T^{miss} and transverse mass of the leptonically decaying W boson, $m_T(W)$, is required to be greater than 60 GeV in order to suppress multijet background. In the case of two b-tags, no further requirement on the E_T^{miss} and transverse mass of the W boson is applied.

After this selection, the $t\bar{t}$ candidate events are reconstructed using a kinematic likelihood fit as described next.

4.3 Reconstruction of the $t\bar{t}$ system

The measurement of the W boson polarisation in $t\bar{t}$ events requires the reconstruction and identification of all $t\bar{t}$ decay products. For this, a kinematic likelihood fitter (KLFitter) [63] is utilised. It maps the four model partons (two b-quarks and the $q\bar{q}'$ pair from a W boson decay) to four reconstructed jets. The numbers of jets used as input for KLFitter can be larger than four. The two jets with the largest output of the b-tagging algorithm together with two (three) remaining jets with the highest p_T were chosen as KLFitter input as this selection leads to the highest reconstruction efficiency for events with four (at least five) jets. For each of the $4! = 24$ ($5! = 120$ for events with at least five jets) possible jet-to-parton permutations, it maximises a likelihood, $\mathcal{L}$, that

---

[2] The jet vertex fraction is defined as the scalar sum of the transverse momenta of a jet's tracks stemming from the primary collision vertex divided by the scalar sum of the transverse momenta of all tracks in a jet.

incorporates Breit–Wigner distributions for the W boson and top quark masses as well as transfer functions mapping the reconstructed jet and lepton energies to parton level or true lepton level, respectively. The expression for the likelihood is given by

$$
\begin{aligned}
\mathscr{L} = {} & BW(m_{q_1 q_2 q_3}|m_t, \Gamma_t) \cdot BW(m_{q_1 q_2}|m_W, \Gamma_W) \\
& \cdot BW(m_{q_4 \ell \nu}|m_t, \Gamma_t) \cdot BW(m_{\ell \nu}|m_W, \Gamma_W) \\
& \cdot W(E_{\text{jet}_1}^{\text{meas}}|E_{q_1}) \cdot W(E_{\text{jet}_2}^{\text{meas}}|E_{q_2}) \cdot W(E_{\text{jet}_3}^{\text{meas}}|E_{q_3}) \cdot (E_{\text{jet}_4}^{\text{meas}}|E_{q_4}) \\
& \cdot W(E_\ell^{\text{meas}}|E_\ell) \cdot W(E^{\text{miss},x}|p_\nu^x) \cdot W(E^{\text{miss},y}|p_\nu^y).
\end{aligned} \tag{3}
$$

where the $BW(m_{ij(k)}|m_{t/W}\Gamma_{t/W})$ terms are the Breit-Wigner functions used to evaluate the mass of composite reconstructed particles (W bosons and top quarks) and $W(E_i^{\text{meas}}|E_j)$ are the transfer functions, with E_i^{meas} being the measured energy of object i and E_j the "true" energy of the reconstructed parton j or true lepton ℓ. The transverse components $p_\nu^{x/y}$ of the neutrino momentum are mapped to the missing transverse momentum $E^{\text{miss},x/y}$ via transfer functions $W(E^{\text{miss},x/y}|p_\nu^{x/y})$. Individual transfer functions for electrons, muons, b-jets, light jets (including c-jets) and missing transverse momentum are used. These transfer functions are obtained from $t\bar{t}$ events simulated with MC@NLO. The top quark decay products are uniquely matched to reconstructed objects to obtain a continuous function describing the relative energy difference between parton and reconstructed level as a function of the parton-level energy. Individual parameterisations are derived for different regions of $|\eta|$. The measurement of the W boson polarisation in the lepton+jets channel is performed for both the top and the anti-top quarks in each event. The anti-down-type quark from the top quark decay (down-type quark from the anti-top quark decay) is used as the hadronic analyser and the charged lepton from the decay of the anti-top quark (charged anti-lepton from the top quark decay) as the leptonic analyser.

Since the likelihood defined in Eq. (3) is invariant under exchange of the W decay products, it needs further extensions to incorporate information related to down-type quarks. This is achieved by multiplying the likelihood by probability distributions of the b-tagging algorithm output as a function of the transverse momentum of the jets. These probability distributions are obtained from MC@NLO for b-quark jets as well as u/c- and d/s-quark jets. Since the W boson decays into a pair of charm and strange quarks in 50% of decays into hadrons, the higher values of the b-tagging algorithm output for the charm quark allows for a separation of the two. This increases the fraction of events with correct matching of the two jets originating from a W boson decay to the corresponding up- and down-quark type jet to 60%, compared to 50% for the case of no separation power. The extended likelihood is normalised with respect to the sum of the extended likelihoods for all 120 (24) permutations and this quantity is called the "event probability". This up- versus down-type quark separation method was established in an ATLAS measurement of the $t\bar{t}$ spin correlation in the lepton+jets channel [64].

The permutation with the largest event probability is chosen. Figure 1a shows the distributions of the logarithm of the likelihood value for the permutation with the highest event probability for simulated $t\bar{t}$ events. Correctly reconstructed events ("$t\bar{t}$ right") peak at high values of the likelihood. Other contributions come from incorrect assignments of jets (i.e. choosing the wrong permutation, "$t\bar{t}$ wrong"), non-reconstructable events where for example a quark is out of the acceptance ("$t\bar{t}$ non-reco") and $t\bar{t}$ events which do not have a lepton+jets topology (such as dileptonic $t\bar{t}$ events, "$t\bar{t}$ background"). In Fig. 1b the corresponding distribution of the event probability is shown. The peak at 0.5 corresponds to events where no separation between up- and down-type quarks is achieved, leading to two permutations with similar
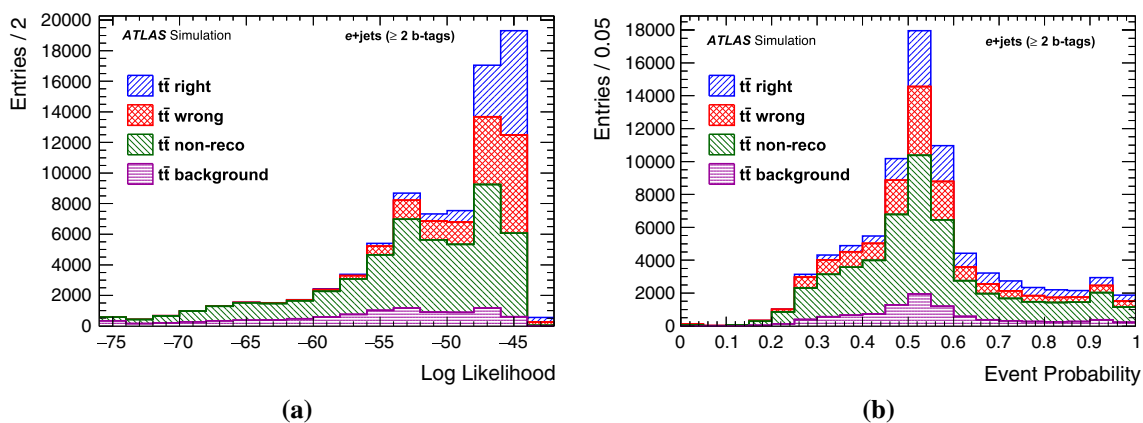

(a)

(b)

Fig. 1 a Logarithm of the likelihood value as output for reconstructed $t\bar{t}$ events of the selected (best) jet-to-parton permutation. **b** Event probability for the selected (best) jet-to-parton permutation. Both distributions show events in the e + jets channel with ≥ 2 b-tags. Events from a

$t\bar{t}$ signal sample are split into events where the $t\bar{t}$ pairs do not decay via the lepton+jets channel ("$t\bar{t}$ background"), events where not all $t\bar{t}$ decay products have been reconstructed ("$t\bar{t}$ non-reco"), as well as correctly ("$t\bar{t}$ right") and incorrectly ("$t\bar{t}$ wrong") reconstructed $t\bar{t}$ systems

Table 1 Expected and observed event yields in the four channels ("e+jets, 1 b-tag", "e+jets, ≥ 2 b-tags", "μ+jets, 1 b-tag" and "μ+jets, ≥ 2 b-tags") after the final event selection including the cut on the reconstruction likelihood. Uncertainties in the normalisation of each sample include systematic uncertainties for the data-driven backgrounds (W+jets and fake leptons) and theory uncertainties for the $t\bar{t}$ signal and the other background sources

Sample	e + jets		μ + jets	
	1 b-tag	$\geq 2b$-tags	1 b-tag	$\geq 2b$-tags
$t\bar{t}$	36,500 ± 2300	36,000 ± 2300	43,600 ± 2800	42,600 ± 2700
Single top	2000 ± 340	974 ± 170	2328 ± 400	1102 ± 190
W+light-jets	600 ± 30	24 ± 1	761 ± 38	45 ± 2
$W + c$	1210 ± 300	54 ± 13	1440 ± 360	51 ± 13
$W + bb/cc$	2730 ± 190	538 ± 38	3520 ± 250	780 ± 55
Z+jets	1200 ± 580	330 ± 160	610 ± 290	158 ± 76
Diboson	220 ± 100	33 ± 16	210 ± 100	37 ± 18
Fake lepton	2270 ± 680	450 ± 130	1750 ± 520	323 ± 97
Total expected	46,700 ± 2600	38,400 ± 2300	54,200 ± 2900	45,100 ± 2800
Data	45,246	40,045	53,747	46,048

event probabilities. High event probability indicates a correct down-type quark reconstruction.

To select the final data sample, the event probability is used to obtain the best jet-to-parton permutation per event. Events are required to have a reconstruction likelihood of $\log \mathscr{L} > -48$ to reject poorly reconstructed $t\bar{t}$ events. The value of $\log \mathscr{L} > -48$ was selected to minimise the expected statistical uncertainty. The fraction of events where all jets were correctly assigned to the corresponding partons out of all events that have the corresponding jets present varies between 45 and 50%. The event yields after the final event selection are presented in Table 1.

Figure 2 shows the likelihood and the event probability as well as the reconstructed $\cos \theta^*$ distribution after the final event selection. Good agreement between data and prediction is achieved.

5 Measurement of the W boson helicity fractions

The W boson helicity fractions F_i are defined as the fraction of produced $t\bar{t}$ events N_i in a given polarisation state divided by all produced $t\bar{t}$ events:

$$F_i = \frac{N_i}{N_0 + N_L + N_R} \quad \text{for} \quad i = 0, L, R. \quad (4)$$

The selection efficiency ϵ_i^{sel} is different for each polarisation state and determines the number of selected events n_i:

$$n_i = \epsilon_i^{\text{sel}} N_i \quad \text{for} \quad i = 0, L, R. \quad (5)$$

Dedicated $t\bar{t}$ signal templates for a specific F_i are created by reweighting the simulated SM $t\bar{t}$ events. These are produced by fitting the $\cos \theta^*$ distribution for the full phase space and calculating per-event weights for each helicity fraction using the functional forms in Eq. (2). Individual templates are created for each lepton flavour and b-tag channel. Figure 3 shows the templates for the μ + jets channel with ≥ 2 b-tags.

In addition to these signal templates, templates are derived for each source j of background events. These are independent of the helicity fractions F_i. Five different background templates are included: three W+jets templates (W+light-jets, Wc+jets and $Wc\bar{c}/b\bar{b}$+jets), a fake-lepton template, and one template for all remaining backgrounds, including contributions from electroweak processes (single top, diboson and Z+jets). The total number of expected events n_{exp} in each channel is then given by

$$n_{\text{exp}} = n_0 + n_L + n_R + n_{W+\text{light}} + n_{W+c} + n_{W+bb/cc}$$
$$+ n_{\text{fake}} + n_{\text{rem.bkg.}}. \quad (6)$$

The signal and background templates are used to perform a likelihood fit with the number of background events $n_{\text{bkg},j}$ and the efficiency corrected signal events N_i as free parameters:

$$\mathscr{L} = \prod_{k=1}^{N_{\text{bins}}} \text{Poisson}(n_{\text{data},k}, n_{\text{exp},k}) \prod_{j=1}^{N_{\text{bkg}}} \frac{1}{\sqrt{2\pi}\sigma_{\text{bkg},j}}$$
$$\times \exp\left(\frac{-(n_{\text{bkg},j} - \hat{n}_{\text{bkg},j})^2}{2\sigma_{\text{bkg},j}^2}\right). \quad (7)$$

Here, $n_{\text{data},k}$ represents the number of events in each bin k. The expected number of background events $\hat{n}_{\text{bkg},j}$ of each background source j and their normalisation uncertainties $\sigma_{\text{bkg},j}$ are used to constrain the fit. The fit parameters scaling the background contributions are treated as correlated across all channels except for the fake-lepton background, which

Fig. 2 Measured and predicted distributions of **a** likelihood and **b** event probability from the kinematic fit and reconstructed $\cos\theta^*$ distribution using **c** the leptonic and **d** the hadronic analysers with ≥ 2 b-tags. The displayed uncertainties represent the Monte Carlo statistical uncertainty as well as the background normalisation uncertainties
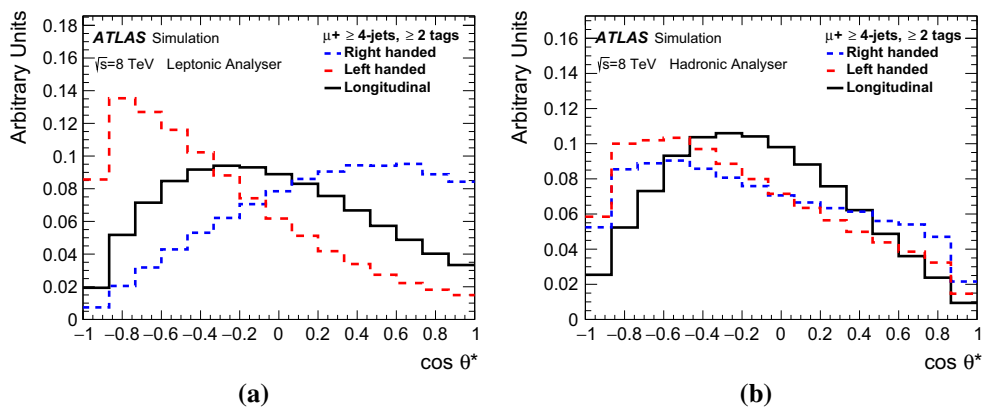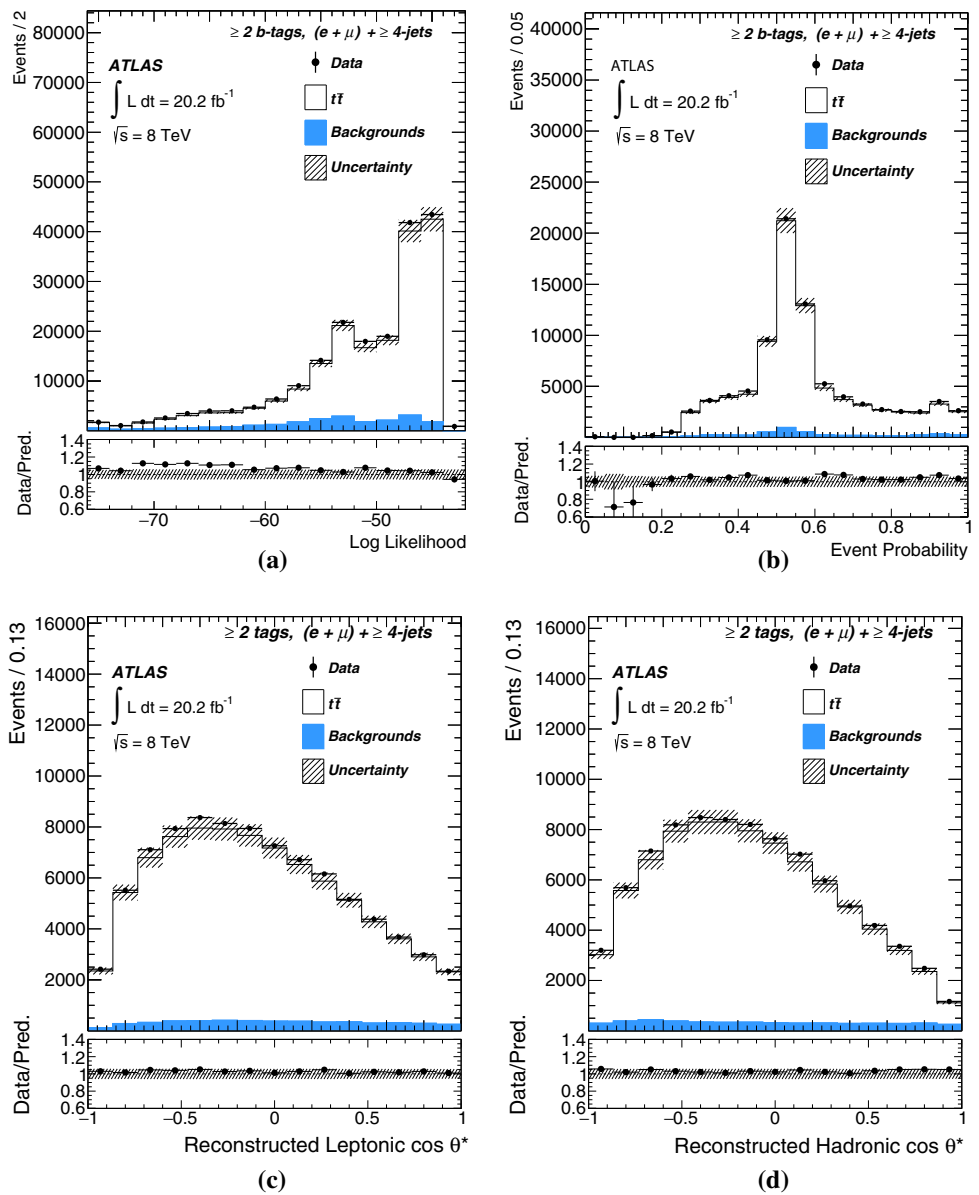

(a)

(b)

(c)

(d)

(a)

(b)

Fig. 3 Templates of the $\cos\theta^*$ distributions for the individual helicity fractions in the $\mu + $ jets channel with ≥ 2 b-tags for the **a** leptonic and **b** hadronic analyser

is uncorrelated across lepton flavours and b-tag regions. The size of the background normalisation uncertainties $\sigma_{\text{bkg},j}$ is described in Sect. 6.

Combined fits of the $\cos \theta^*$ distributions using up to four different channels (e + jets and μ + jets, both with 1 b-tag or $\geq$ 2 b-tags) are performed for the leptonic and hadronic analyser individually. For each channel, individual templates of the signal and backgrounds are utilised. The combination leading to the lowest total uncertainty is used to quote the result. The helicity fractions are obtained from the fitted values of n_i using Eqs. 4–6. The fit method is validated using pseudo-experiments varying F_0 over the range [0.4, 1.0], F_L over the range [0.15, 0.45] and F_R over the range [−0.15, 0.15]. For each set, the unitarity constraint ($F_0 + F_L + F_R = 1$) is imposed. No bias is observed.

The uncertainties in the helicity fractions obtained from the fit include both the statistical uncertainty of the data and the systematic uncertainty of the background normalisations. For the leptonic analyser, the most sensitive results are obtained for the two-channel combination (electron + muon) in the ≥ 2 b-tags region. Adding further channels increases the total systematic uncertainty, in particular due to uncertainties in the b-tagging, which do not compensate with the decrease in the statistical uncertainty. For the hadronic analyser, the four-channel combination (including both the 1 b-tag and ≥ 2 b-tags regions) improves the sensitivity compared to the two-channel combination. For each source of systematic uncertainty, modified pseudo-data templates are created and evaluated via ensemble testing. The differences between the mean helicity fractions measured using the nominal templates and those varied to reflect systematic errors are quoted as systematic uncertainty. Systematic uncertainties from different sources, described in the following section, are treated as uncorrelated.

6 Systematic uncertainties

Systematic uncertainties from several sources can affect the normalisation of the signal and background and/or the shape of the $\cos \theta^*$ distribution. Correlations of a given systematic uncertainty are maintained across processes and channels, unless otherwise stated. The impact of uncertainties from the various sources is determined using a frequentist method based on the generation of pseudo-experiments.

6.1 Uncertainties associated with reconstructed objects

Different sources of systematic uncertainty affect the reconstructed objects used in this analyses. All these sources, described in the following, are propagated to changes in the shape of the $\cos \theta^*$ distributions.

Uncertainties associated with the lepton selection arise from the trigger, reconstruction, identification and isolation efficiencies, as well as the lepton momentum scale and resolution. They are estimated from $Z \to \ell^+ \ell^- (\ell = e, \mu)$, $J/\psi \to \ell^+ \ell^-$ and $W \to e\nu$ processes in data and in simulated samples using tag-and-probe techniques described in Refs. [65–69]. Since small differences are observed between data and simulation, correction factors and their related uncertainties are considered to account for these differences. The effect of these uncertainties is propagated through the analysis and represent a minor source of uncertainty in this measurement.

Uncertainties associated with the jet selection arise from the jet energy scale, jet energy resolution, jet vertex fraction requirement and jet reconstruction efficiency. The jet energy scale and its uncertainty are derived combining information from test-beam data, LHC collision data, and simulation [58]. The jet energy scale uncertainty is split into 22 uncorrelated sources that have different jet p_T and η dependencies and are treated independently in this analysis. The uncertainty related to the jet energy resolution is estimated by smearing the energy of jets in simulation by the difference between the jet energy resolutions for data and simulation [70]. The efficiency for each jet to satisfy the jet vertex fraction requirement is measured in $Z \to \ell^+ \ell^- + 1$-jet events in data and simulation [71]. The corresponding uncertainty is evaluated in the analysis by changing the nominal jet vertex fraction cut value and repeating the analysis using the modified cut value [72]. The jet reconstruction efficiency is found to be about 0.2% lower in simulation than in data for jets below 30 GeV and consistent with data for higher jet p_T. All jet-related kinematic variables (including the missing transverse momentum) are recomputed by removing randomly 0.2% of the jets with p_T below 30 GeV and the event selection is repeated.

Since the b-tagging efficiencies and misidentification rates are not modelled satisfactorily in MC simulation, all jets are assigned a specific p_T- and η-dependent scale factor to account for this difference. The uncertainties in these scale factors are propagated to the measured value.

An additional uncertainty is assigned due to the extrapolation of the b-tagging efficiency measurement to the high-p_T region. Twelve uncertainties are considered for the light-jet tagging, all depending on jet p_T and η. These systematic uncertainties are taken as uncorrelated.

The uncertainties from the energy scale and resolution corrections for leptons and jets are propagated into the E_T^{miss} calculation. Additional uncertainties are added to account for contributions from energy deposits not associated with any jet and due to soft-jets (7 GeV $< p_T <$ 20 GeV), and are treated as fully correlated with each other. The uncertainty in the description of extra energy deposited due to pile-up interactions is treated as a separate E_T^{miss} scale uncertainty.

This uncertainty has a negligible effect on the measured W boson helicity fractions.

6.2 Uncertainties in signal modelling

The uncertainties in the signal modelling affect the kinematic properties of simulated $t\bar{t}$ events and thus the acceptance and the shape of the reconstructed $\cos\theta^*$ distribution.

To assess the impact of the different parton shower and hadronisation models, the POWHEG+HERWIG sample is compared to a POWHEG+PYTHIA sample and the symmetrised difference is taken as a systematic uncertainty. Similarly, an uncertainty due to the matrix element (ME) MC event generator choice for the hard process is estimated by comparing events produced by POWHEG-BOX and MC@NLO, both interfaced to HERWIG for showering and hadronisation. The uncertainties due to QCD initial- and final-state radiation (ISR/FSR) modelling are estimated using two POWHEG+PYTHIA samples with varied parameters producing more and less radiation. The larger of the changes due to the two variations is taken and symmetrised.

The uncertainty in the $t\bar{t}$ signal due to the PDF choice is estimated following the PDF4LHC recommendations [73]. It takes into account the differences between three PDF sets: CT10 NLO, MSTW2008 68% CL NLO and NNPDF 2.3 NLO [74]. The final PDF uncertainty is an envelope of an intra-PDF uncertainty, which evaluates the changes due to the variation of different PDF parameters within a single PDF error set, and an inter-PDF uncertainty, which evaluates differences between different PDF sets. Each PDF set has a prescription to evaluate an overall uncertainty using its error sets: symmetric Hessian in the case of CT10, asymmetric Hessian for MSTW and sample standard deviation in the NNPDF case. Half the width of the envelope of the three estimates is taken as the PDF systematic uncertainty.

The effect of the uncertainty in the top quark mass is estimated using MC samples with different input top masses for the signal process. The dependence of the obtained helicity fractions on the top quark mass is fitted with a linear function. The uncertainties in the helicity fractions are obtained from the slopes multiplied by the uncertainty in the top quark mass of 172.84 ± 0.70 GeV [45] measured by ATLAS at $\sqrt{s} = 8$ TeV.

6.3 Uncertainties in background modelling

The different flavour samples of the W+jets background are scaled by data-driven calibration factors [49] as explained in Sect. 3. All sources of uncertainty on the correction factors other than normalisation (e.g. associated with the objects identification, reconstruction and calibration, etc.) are propagated to the W+jets estimation. Their normalisation uncertainty (5% for W+light-jets, 25% for W+c-jets and 7%

for W+bb/cc) is taken into account in the likelihood fit as explained in Sect. 5.

A relative uncertainty of 30%, estimated using various control regions in the matrix method calculation [52], is used for the fake-lepton contribution.

For single top quark production, a normalisation uncertainty of 17% is assumed, which takes into account the weighted average of the theoretical uncertainties in s-, t- and Wt-channel production (+5/−4%) as well as additional uncertainties due to variations in the amount of initial- and final-state radiation and the extrapolation to high jet multiplicity. The uncertainty in the single-top background shape is assessed by comparing Wt-channel Monte Carlo samples generated using alternative methods to take into account Wt and $t\bar{t}$ diagrams interference: diagram removal and diagram subtraction [39].

An overall normalisation uncertainty of 48% is applied to Z+jets and diboson contributions. It takes into account a 5% uncertainty in the theoretical (N)NLO cross-section as well as the uncertainty associated with the extrapolation to high jet multiplicity (24% per jet).

All normalisation uncertainties are included in the fit of the W boson helicity fractions via priors for the background yields. While the W+jets and fake-lepton uncertainties are included directly, the uncertainty in the total remaining background from other sources is combined to 16% (17%) in the ≥ 2 b-tags regions (1 b-tag + ≥ 2 b-tags regions) by adding the uncertainties in the theoretical cross-sections of the single top quark, diboson and Z+jets contributions in quadrature. The uncertainty in the shape of the W+jets background is considered by jet flavour decomposition. Further background shape uncertainties were evaluated and found to be negligible.

6.4 Other uncertainties

The uncertainty associated with the limited number of MC events in the signal and background templates is evaluated by performing pseudo-experiments on MC events.

The impact of the 1.9% luminosity uncertainty [75] is found to be negligible since the background normalisations are constrained in the fit.

7 Results

The measured W boson helicity fractions obtained using the leptonic analyser in semileptonic $t\bar{t}$ events with ≥ 2 b-tags are presented in Table 2.

By construction, the individual fractions sum up to one. The F_0 value is anti-correlated with both F_L and F_R ($\rho_{F_0,F_L} = -0.55$, $\rho_{F_0,F_R} = -0.75$), and F_L and F_R are positively correlated ($\rho_{F_L,F_R} = +0.16$). The quoted values correspond to the total correlation coefficient, consid-

Table 2 Measured W boson helicity fractions obtained from the leptonic analyser including the statistical uncertainty from the fit and the background normalisation as well as the systematic uncertainty

Leptonic analyser (≥ 2 b-tags)

$F_0 = 0.709 \pm 0.012$ (stat.+bkg. norm.) $^{+0.015}_{-0.014}$ (syst.)

$F_L = 0.299 \pm 0.008$ (stat.+bkg. norm.) $^{+0.013}_{-0.012}$ (syst.)

$F_R = -0.008 \pm 0.006$ (stat.+bkg. norm.) ± 0.012 (syst.)

Table 3 Measured W boson helicity fractions for the hadronic analyser including the statistical uncertainty from the fit and the background normalisation as well as the systematic uncertainty

Hadronic analyser (1 b-tag + ≥ 2 b-tags)

$F_0 = 0.659 \pm 0.010$ (stat.+bkg. norm.) $^{+0.052}_{-0.054}$ (syst.)

$F_L = 0.281 \pm 0.021$ (stat.+bkg. norm.) $^{+0.063}_{-0.067}$ (syst.)

$F_R = 0.061 \pm 0.022$ (stat.+bkg. norm.) $^{+0.101}_{-0.108}$ (syst.)
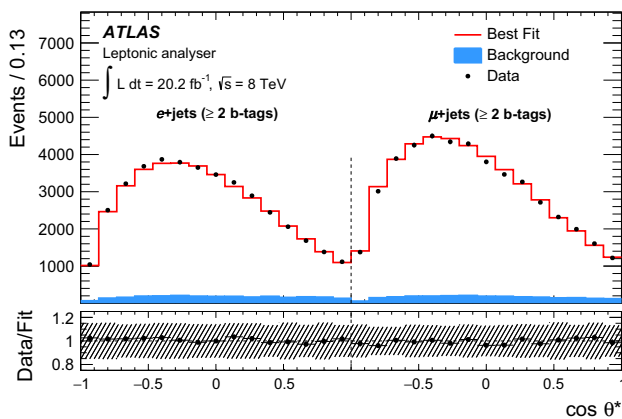
ering statistical and systematic uncertainties. These results are the most precise W boson helicity fractions measured so far and are consistent with the SM predictions given at NNLO accuracy [3]. The inclusion of single b-tag regions does not improve the sensitivity, due to larger systematic uncertainties.

The W boson helicity fractions obtained using the hadronic analyser of semileptonic $t\bar{t}$ events with 1 b-tag and $\geq 2b$-tags are given in Table 3. Using the hadronic analyser, the correlations between the helicity fraction are $\rho_{F_0,F_L} = 0.56$, $\rho_{F_0,F_R} = -0.91$ and $\rho_{F_L,F_R} = -0.92$. The large anticorrelation between F_L and F_R is a consequence of the low separation power between the up- and down-type quark from the W decay and the resulting similar shapes of the templates of F_L and F_R (see Fig. 3). The results obtained with the two analysers agree well. The combination of leptonic and hadronic analysers has been tested and, despite the improvement in the statistical uncertainty, it does not improve the total uncertainty.

Figure 4 shows, separately for the e+jets and μ+jets channels, the distributions of $\cos\theta^*$ from the leptonic analyser. The distributions for the hadronic analyser are presented in Fig. 5. The uncertainty band in the data-to-best-fit ratio represents the statistical and background normalisation uncertainty. The deviations observed in the ratio are covered by the systematic uncertainties. The peak at $\cos\theta^* \approx -0.7$ as seen in the single b-tag channels in Fig. 5 is caused by misreconstructed events. A missing second b-tag increases the probability of swapping the b-quark jet from the top quark decay with the up-type quark jet from the W decay.

The contributions of the various systematic uncertainties are quoted in Table 4. In the case of the leptonic analyser, the dominant contributions come from the jet energy scale and resolution and the statistical error in the MC templates. For the hadronic analyser, the systematic uncertainties are larger.
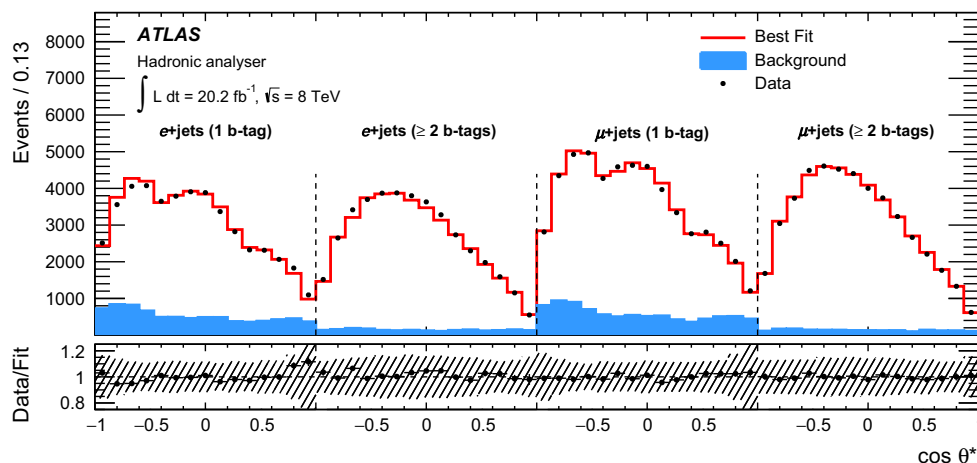

Fig. 4 Post-fit distribution of $\cos\theta^*$ for the leptonic analyser with ≥ 2 b-tags, in which a two-channel combination is performed (electron and muon). The uncertainty band represents the total uncertainty in the fit result

Fig. 5 Post-fit distribution of $\cos\theta^*$ for the hadronic analyser, in which the combination of four channels is performed (electron and muon, with exactly 1 b-tag and ≥ 2 b-tags). The uncertainty band represents the total uncertainty in the fit result

Table 4 Summary of systematic and statistical uncertainties for the measurements obtained using the leptonic (left) and the hadronic (right) analysers. The numbers in the last row (Stat. + bkg. norm) correspond to the statistical uncertainty of the fit, including the normalisation uncertainties in the background yields

Uncertainty	Leptonic, ≥ 2 b-tags			Hadronic, $1 + \geq 2$ b-tags		
	F_0	F_L	F_R	F_0	F_L	F_R
Reconstructed objects						
Electron	+0.0028	+0.0018	+0.0011	+0.0025	+0.0028	+0.0051
	−0.0030	−0.0020	−0.0011	−0.0021	−0.0038	−0.0058
Muon	+0.0024	+0.0013	+0.0010	+0.0026	+0.0046	+0.0072
	−0.0029	−0.0015	−0.0015	−0.0037	−0.0035	−0.0072
Jet energy scale	+0.0063	+0.0028	+0.0037	+0.0069	+0.012	+0.014
	−0.0033	−0.0025	−0.0014	−0.0070	−0.008	−0.005
Jet energy resolution	+0.0062	+0.0048	+0.0072	+0.027	+0.033	+0.057
	−0.0059	−0.0018	−0.0067	−0.031	−0.041	−0.071
Jet vertex fraction	+0.0036	+0.0019	+0.0017	+0.013	+0.0012	+0.011
	−0.0017	−0.0013	−0.0006	−0.009	−0.0046	−0.005
Jet reconstruction efficiency	+0.0002	<0.0001	+0.0002	+0.0008	+0.0004	+0.0011
	−0.0002	<0.0001	−0.0002	−0.0008	−0.0004	−0.0011
b-tagging	+0.0017	+0.0012	+0.0011	+0.029	+0.013	+0.034
	−0.0021	−0.0013	−0.0012	−0.031	−0.014	−0.035
Sum reconstructed objects	+0.010	+0.0064	+0.0085	+0.043	+0.038	+0.069
	−0.008	−0.0044	−0.0072	−0.045	−0.044	−0.080
Signal modelling						
Showering and hadronisation	±0.0019	±0.0019	±0.0037	±0.015	±0.001	±0.014
ME event generator	±0.0025	±0.0032	±0.0057	±0.016	±0.024	±0.040
ISR/FSR	±0.0033	±0.0058	±0.0034	±0.018	±0.039	±0.057
PDF	±0.0033	±0.0042	±0.0009	±0.0010	±0.0020	±0.0020
Top quark mass	±0.0017	±0.0050	±0.0033	±0.0033	±0.0100	±0.0068
Sum signal modelling	±0.0058	±0.0094	±0.0082	±0.028	±0.047	±0.072
Method uncertainty						
Template statistics	±0.0091	±0.0056	±0.0044	±0.0076	±0.016	±0.016
Total uncertainty						
Total systematic	+0.015	+0.013	+0.013	+0.052	+0.063	+0.100
	−0.014	−0.012	−0.012	−0.054	−0.067	−0.110
Stat. + bkg. norm	±0.012	±0.008	±0.006	±0.010	±0.021	±0.022

Including the 1 b-tag region aids in reducing the error. One of the main contributions is the b-tagging uncertainty, affecting both the event selection and b-tag categorisation, as well as the up- vs down-type quark separation. Other major contributions come from the jet energy resolution and the modelling of $t\bar{t}$ events (initial- and final-state radiation, parton showering and hadronisation, and Monte Carlo event generator choice for the matrix elements).

Within the effective field theory framework [76], the Wtb decay vertex can be parameterised in terms of anomalous couplings as shown in Eq. (1). Limits on these anomalous left- and right-handed vector and tensor couplings are set using the EFTfitter tool [77] and the model of [76]. The anomalous couplings are assumed to be real, corresponding to the CP-conserving case. As the W helicity fractions only allow the ratios of couplings to be constrained, the value of V_L is fixed to the Standard Model prediction of one. The correlations of systematic uncertainties are taken into account. Figure 6 shows the limits on g_L and g_R couplings while V_L and V_R are fixed to their SM values, as well as V_R and g_R limits, where the other couplings are fixed to their SM values. The intervals are obtained using the leptonic analyser since it provides the most sensitive results. Table 5 shows the 95% confidence level (CL) intervals for each anomalous coupling while fixing all others to their SM value. These limits correspond to the set of smallest intervals containing 95% of
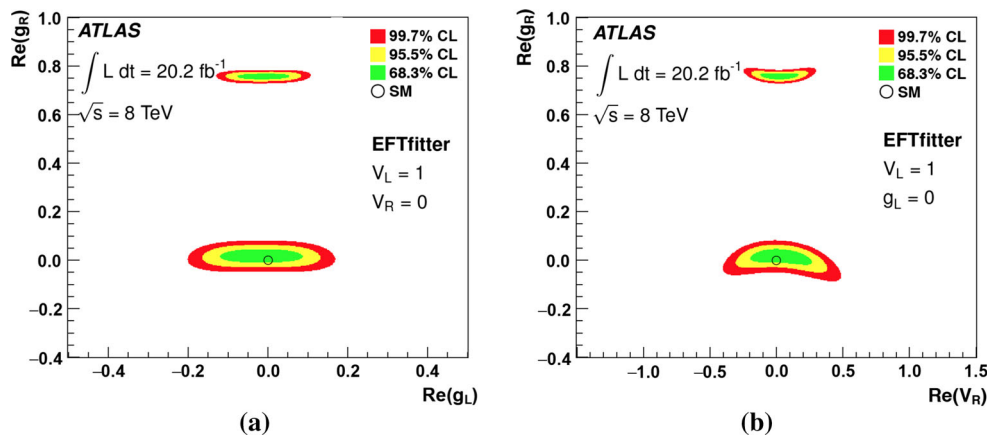
Fig. 6 a Limits on the anomalous left- and right-handed tensor couplings of the Wtb decay vertex as obtained from the measured W boson helicity fractions from the leptonic analyser. **b** Limits on the right-handed vector and tensor coupling. As the couplings are assumed to be real, the real part corresponds to the magnitude. Unconsidered couplings are fixed to their SM values

Table 5 Allowed ranges for the anomalous couplings V_R, g_L, and g_R at 95% CL. The limits are derived using the measured W helicity fractions using the leptonic analyser for events with ≥ 2 b-tags (combination of the two channels, electron and muon)

Coupling	95% CL interval
V_R	$[-0.24, 0.31]$
g_L	$[-0.14, 0.11]$
g_R	$[-0.02, 0.06]$, $[0.74, 0.78]$

the marginalised posterior distribution for the corresponding parameter.

Similar limits on the anomalous couplings were derived by both the ATLAS and CMS experiments using the measured helicity fractions of W bosons [10,11]. Complementary limits can be set by other measurements: the allowed region of $g_R \approx 0.75$ is excluded by measurements of the t-channel single top quark production [77–80] which also constrains V_L. The branching fraction of $\bar{B} \to X_s\gamma$ allow more stringent limits to be set on g_L and V_R [81].

8 Conclusion

The longitudinal, left- and right-handed W boson helicity fractions are measured using the angle between the charged lepton (down-type quark) and the reversed b-quark direction in the W boson rest frame for leptonically (hadronically) decaying W bosons from $t\bar{t}$ decays. A data set corresponding to 20.2 fb^{-1} of pp collisions at the LHC with a centre-of-mass energy of $\sqrt{s} = 8$ TeV, recorded by the ATLAS experiment, is analysed. Events are required to include one isolated electron or muon and at least four jets, with at least one of them tagged as a b-jet. Events are recon-

structed using a kinematic likelihood fit based on mass constraints for the top quarks and W bosons. It utilises the weight of the b-jet tagging algorithm to further separate the up- and down-type quarks from the hadronically decaying W bosons. The fractions for left-handed, right-handed and longitudinally polarised W bosons are found to be $F_0 = 0.709 \pm 0.012$ (stat.+bkg. norm.) ± 0.015 (syst.), $F_L = 0.299 \pm 0.008$ (stat.+bkg. norm.) ± 0.013 (syst.) and $F_R = -0.008 \pm 0.006$ (stat.+bkg. norm.) ± 0.012 (syst.). These results constitute the most precise measurement of the W helicity fractions in $t\bar{t}$ events to date and are in good agreement with the Standard Model predictions within uncertainties. Using these results, limits on anomalous couplings of the Wtb vertex are set.

References

1. CDF Collaboration, F. Abe et al., Observation of top quark production in $\bar{p}p$ collisions. Phys. Rev. Lett. **74**, 2626 (1995). doi:10. 1103/PhysRevLett.74.2626. arXiv: hep-ex/9503002

2. D0 Collaboration, S. Abachi et al., Search for high mass top quark production in $p\bar{p}$ collisions at $\sqrt{s}$ = 1.8 TeV, Phys. Rev. Lett. **74**, 2422 (1995). doi:10.1103/PhysRevLett.74.2422. arXiv: hep--ex/9411001

3. A. Czarnecki, J.G. Korner, J.H. Piclum, Helicity fractions of W bosons from top quark decays at NNLO in QCD. Phys. Rev. D **81**, 111503 (2010). doi:10.1103/PhysRevD.81.111503. arXiv: 1005.2625 [hep-ph]

4. W. Buchmuller, D. Wyler, Effective Lagrangian analysis of new interactions and flavor conservation. Nucl. Phys. B **268**, 621 (1986). doi:10.1016/0550-3213(86)90262-2

5. J.A. Aguilar-Saavedra, A minimal set of top anomalous couplings. Nucl. Phys. B **812**, 181 (2009). doi:10.1016/j.nuclphysb.2008.12. 012. arXiv:0811.3842 [hep-ph]

6. C. Zhang, S. Willenbrock, Effective-field-theory approach to top-quark production and decay. Phys. Rev. D **83**, 034006 (2011). doi:10.1103/PhysRevD.83.034006. arXiv:1008.3869 [hep-ph]

7. CDF and D0 Collaborations, T. Aaltonen et al., Combination of CDF and D0 measurements of the W boson helicity in top quark decays. Phys. Rev. D **85**, 071106 (2012). doi:10.1103/PhysRevD. 85.071106. arXiv:1202.5272 [hep-ex]

8. CDF Collaboration, T. Aaltonen et al., Measurement of W-Boson Polarization in Top-quark Decay in $p\bar{p}$ Collisions at $\sqrt{s}$ = 1.96 TeV. Phys. Rev. Lett **105**, 042002 (2010). doi:10.1103/PhysRevLett. 105.042002. arXiv:1003.0224 [hep-ex]

9. D0 Collaboration, V.M. Abazov et al., Measurement of the W boson helicity in top quark decays using 5.4 fb^{-1} of $p\bar{p}$ collision data. Phys. Rev. D **83**, 032009 (2011). doi:10.1103/PhysRevD.83. 032009. arXiv:1011.6549 [hep-ex]

10. ATLAS Collaboration, Measurement of the W boson polarization in top quark decays with the ATLAS detector. JHEP **06**, 088 (2012). doi:10.1007/JHEP06(2012)088. arXiv:1205.2484 [hep-ex]

11. CMS Collaboration, Measurement of the W boson helicity fractions in the decays of top quark pairs to lepton + jets final states produced in pp collisions at $\sqrt{s}$ = 8 TeV. Phys. Lett. B **762**, 512 (2016). doi:10.1016/j.physletb.2016.10.007. arXiv:1605.09047 [hep-ex]

12. ATLAS Collaboration, The ATLAS experiment at the CERN large hadron collider. JINST **3**, S08003 (2008). doi:10.1088/1748-0221/ 3/08/S08003

13. ATLAS Collaboration, The ATLAS simulation infrastructure. Eur. Phys. J. C **70**, 823 (2010). doi:10.1140/epjc/s10052-010-1429-9. arXiv:1005.4568 [hep-ex]

14. S. Agostinelli et al., GEANT4: a simulation toolkit. Nucl. Instrum. Methods A **506**, 250 (2003). doi:10.1016/S0168-9002(03)01368-8

15. ATLAS Collaboration, The simulation principle and performance of the ATLAS fast calorimeter simulation FastCaloSim. ATL-PHYS-PUB-2010-013,2010, http://cds.cern.ch/record/1300517

16. P. Nason, A new method for combining NLO QCD with shower Monte Carlo algorithms. JHEP **11**, 040 (2004). doi:10.1088/ 1126-6708/2004/11/040. arXiv:hep-ph/0409146

17. S. Frixione, P. Nason, G. Ridolfi, A positive-weight next-to-leading-order Monte Carlo for heavy flavour hadroproduction. JHEP **09**, 126 (2007). doi:10.1088/1126-6708/2007/09/126. arXiv:0707.3088 [hep-ph]

18. S. Frixione, P. Nason, C. Oleari, Matching NLO QCD computations with Parton shower simulations: the POWHEG method. JHEP **11**, 070 (2007). doi:10.1088/1126-6708/2007/11/070. arXiv:0709.2092 [hep-ph]

19. S. Alioli, P. Nason, C. Oleari, E. Re, A general framework for implementing NLO calculations in shower Monte Carlo programs: the POWHEG BOX. JHEP **06**, 043 (2010). doi:10.1007/ JHEP06(2010)043. arXiv:1002.2581 [hep-ph]

20. H.-L. Lai et al., New parton distributions for collider physics. Phys. Rev. D **82**, 074024 (2010). doi:10.1103/PhysRevD.82.074024. arXiv:1007.2241 [hep-ph]

21. T. Sjöstrand, S. Mrenna, P.Z. Skands, PYTHIA 6.4 physics and manual. JHEP **05**, 026 (2006). doi:10.1088/1126-6708/2006/05/ 026. arXiv:hep-ph/0603175

22. J. Pumplin et al., New generation of parton distributions with uncertainties from global QCD analysis. JHEP **07**, 012 (2002). doi:10. 1088/1126-6708/2002/07/012. arXiv:hep-ph/0201195

23. P.Z. Skands, Tuning Monte Carlo generators: the perugia tunes. Phys. Rev. D **82**, 074018 (2010). doi:10.1103/PhysRevD.82. 074018. arXiv:1005.3457 [hep-ph]

24. M. Cacciari, M. Czakon, M. Mangano, A. Mitov, P. Nason, Top-pair production at hadron colliders with next-to-next-to-leading logarithmic soft-gluon resummation. Phys. Lett. B **710**, 612 (2012). doi:10.1016/j.physletb.2012.03.013. arXiv:1111.5869 [hep-ph]

25. M. Beneke, P. Falgari, S. Klein, C. Schwinn, Hadronic top-quark pair production with NNLL threshold resummation. Nucl. Phys. B **855**, 695 (2012). doi:10.1016/j.nuclphysb.2011.10.021. arXiv:1109.1536 [hep-ph]

26. P. Bärnreuther, M. Czakon, A. Mitov, Percent level precision physics at the tevatron: first genuine NNLO QCD corrections to $q\bar{q} \rightarrow t\bar{t} + X$. Phys. Rev. Lett. **109**, 132001 (2012). doi:10.1103/ PhysRevLett.109.132001. arXiv:1204.5201 [hep-ph]

27. M. Czakon, A. Mitov, NNLO corrections to top pair production at hadron colliders: the quark-gluon reaction. JHEP **01**, 080 (2013). doi:10.1007/JHEP01(2013)080. arXiv:1210.6832 [hep-ph]

28. M. Czakon, A. Mitov, NNLO corrections to top-pair production at hadron colliders: the all-fermionic scattering channels. JHEP **12**, 054 (2012). doi:10.1007/JHEP12(2012)054. arXiv:1207.0236 [hep-ph]

29. M. Czakon, P. Fiedler, A. Mitov, Total top-quark pair-production cross section at hadron colliders through $O(\alpha_S^4)$. Phys. Rev. Lett. **110**, 252004 (2013). doi:10.1103/PhysRevLett.110.252004. arXiv:1303.6254 [hep-ph]

30. M. Czakon, A. Mitov, Top++: a program for the calculation of the top-pair cross-section at hadron colliders. Comput. Phys. Commun. **185**, 2930 (2014). doi:10.1016/j.cpc.2014.06.021. arXiv:1112.5675 [hep-ph]

31. G. Corcella et al., HERWIG 6: an event generator for hadron emission reactions with interfering gluons (including supersymmetric processes). JHEP **01**, 010 (2001). doi:10.1088/1126-6708/2001/01/010. arXiv:hep-ph/0011363

32. J.M. Butterworth, J.R. Forshaw, M.H. Seymour, Multiparton interactions in photoproduction at HERA. Z. Phys. C **72**, 637 (1996). doi:10.1007/BF02909195, doi:10.1007/s002880050286. arXiv:hep-ph/9601371

33. S. Frixione, B.R. Webber, Matching NLO QCD computations and parton shower simulations. JHEP **06**, 029 (2002). doi:10.1088/1126-6708/2002/06/029. arXiv:hep-ph/0204244

34. S. Frixione, P. Nason, B.R. Webber, Matching NLO QCD and parton showers in heavy flavor production. JHEP **08**, 007 (2003). doi:10.1088/1126-6708/2003/08/007. arXiv:hep-ph/0305252

35. ATLAS Collaboration, New ATLAS event generator tunes to 2010 data. ATL-PHYS-PUB-2011-008, 2011. http://cds.cern.ch/record/1345343

36. ATLAS Collaboration, Measurement of $t\bar{t}$ production with a veto on additional central jet activity in pp collisions at $\sqrt{s} = 7$ TeV using the ATLAS detector. Eur. Phys. J. C **72**, 2043 (2012). doi:10.1140/epjc/s10052-012-2043-9. arXiv:1203.5015 [hep-ex]

37. S. Alioli, P. Nason, C. Oleari, E. Re, NLO single-top production matched with shower in POWHEG: s- and t-channel contributions. JHEP **09**, 111 (2009). [Erratum: JHEP **02**, 011 (2010)]. doi:10.1007/JHEP02(2010)011, doi:10.1088/1126-6708/2009/09/111. arXiv:0907.4076 [hep-ph]

38. E. Re, Single-top Wt-channel production matched with parton showers using the POWHEG method. Eur. Phys. J. C **71**, 1547 (2011). doi:10.1140/epjc/s10052-011-1547-z. arXiv:1009.2450 [hep-ph]

39. S. Frixione, E. Laenen, P. Motylinski, B.R. Webber, C.D. White, Single-top hadroproduction in association with a W boson. JHEP **07**, 029 (2008). doi:10.1088/1126-6708/2008/07/029. arXiv:0805.3067 [hep-ph]

40. N. Kidonakis, Next-to-next-to-leading-order collinear and soft gluon corrections for t-channel single top quark production. Phys. Rev. D **83**, 091503 (2011). doi:10.1103/PhysRevD.83.091503. arXiv:1103.2792 [hep-ph]

41. N. Kidonakis, NNLL resummation for s-channel single top quark production. Phys. Rev. D **81**, 054028 (2010). doi:10.1103/PhysRevD.81.054028. arXiv:1001.5034 [hep-ph]

42. N. Kidonakis, Two-loop soft anomalous dimensions for single top quark associated production with a W- or H-. Phys. Rev. D **82**, 054018 (2010). doi:10.1103/PhysRevD.82.054018. arXiv:1005.4451 [hep-ph]

43. A.D. Martin, W.J. Stirling, R.S. Thorne, G. Watt, Parton distributions for the LHC. Eur. Phys. J. C **63**, 189 (2009). doi:10.1140/epjc/s10052-009-1072-5. arXiv:0901.0002 [hep-ph]

44. A.D. Martin, W.J. Stirling, R.S. Thorne, G. Watt, Uncertainties on alpha(S) in global PDF analyses and implications for predicted hadronic cross sections. Eur. Phys. J. C **64**, 653 (2009). doi:10.1140/epjc/s10052-009-1164-2. arXiv:0905.3531 [hep-ph]

45. ATLAS Collaboration, Measurement of the top quark mass in the $t\bar{t} \rightarrow$ dilepton channel from $\sqrt{s} = 8$ TeV ATLAS data. Phys. Lett. B **761**, 350 (2016). doi:10.1016/j.physletb.2016.08.042. arXiv:1606.02179 [hep-ex]

46. M.L. Mangano, M. Moretti, F. Piccinini, R. Pittau, A.D. Polosa, ALPGEN, a generator for hard multiparton processes in hadronic collisions. JHEP **07**, 001 (2003). doi:10.1088/1126-6708/2003/07/001. arXiv:hep-ph/0206293

47. M.L. Mangano, M. Moretti, R. Pittau, Multijet matrix elements and shower evolution in hadronic collisions: $Wb\bar{b} + n$ jets as a case study. Nucl. Phys. B **632**, 343 (2002). doi:10.1016/S0550-3213(02)00249-3. arXiv:hep-ph/0108069

48. K. Melnikov, F. Petriello, Electroweak gauge boson production at hadron colliders through O(alpha(s)**2). Phys.

Rev. D **74**, 114017 (2006). doi:10.1103/PhysRevD.74.114017. arXiv:hep-ph/0609070

49. ATLAS Collaboration, Measurement of the charge asymmetry in top-quark pair production in the lepton-plus-jets final state in pp collision data at $\sqrt{s} = 8$ TeV with the ATLAS detector. Eur. Phys. J. C **76**, 87 (2016). doi:10.1140/epjc/s10052-016-3910-6. arXiv:1509.02358 [hep-ex]

50. T. Gleisberg et al., Event generation with SHERPA 1.1. JHEP **02**, 007 (2009). doi:10.1088/1126-6708/2009/02/007. arXiv:0811.4622 [hep-ph]

51. J.M. Campbell, R.K. Ellis, An Update on vector boson pair production at hadron colliders. Phys. Rev. D **60**, 113006 (1999). doi:10.1103/PhysRevD.60.113006. arXiv:hep-ph/9905386

52. ATLAS Collaboration, Estimation of non-prompt and fake lepton backgrounds in final states with top quarks produced in proton–proton collisions at $\sqrt{s} = 8$ TeV with the ATLAS Detector. ATLAS-CONF-2014-058, 2014. http://cds.cern.ch/record/1951336

53. ATLAS Collaboration, Electron efficiency measurements with the ATLAS detector using the 2012 LHC proton–proton collision data. ATLAS-CONF-2014-032, 2014. http://cds.cern.ch/record/1706245

54. M. Cacciari, G.P. Salam, G. Soyez, The anti-k_t jet clustering algorithm. JHEP **04**, 063 (2008). doi:10.1088/1126-6708/2008/04/063. arXiv:0802.1189 [hep-ph]

55. M. Cacciari, G.P. Salam, Dispelling the N^3 myth for the k_t jet-finder. Phys. Lett. B **641**, 57 (2006). doi:10.1016/j.physletb.2006.08.037. arXiv:hep-ph/0512210

56. W. Lampl et al., Calorimeter Clustering Algorithms: Description and Performance. ATL-LARG-PUB-2008-002, 2008. http://cds.cern.ch/record/1099735

57. C. Cojocaru et al., Hadronic calibration of the ATLAS liquid argon end-cap calorimeter in the pseudorapidity region $1.6<|\eta|<1.8$ in beam tests. Nucl. Instrum. Methods A **531**, 481 (2004). doi:10.1016/j.nima.2004.05.133. arXiv:physics/0407009

58. ATLAS Collaboration, Jet energy measurement and its systematic uncertainty in proton–proton collisions at $\sqrt{s} = 7$ TeV with the ATLAS detector. Eur. Phys. J. C **75**, 17 (2015). doi:10.1140/epjc/s10052-014-3190-y. arXiv:1406.0076 [hep-ex]

59. ATLAS Collaboration, Performance of b-jet identification in the ATLAS experiment. JINST **11**, P04008 (2016). doi:10.1088/1748-0221/11/04/P04008. arXiv:1512.01094 [hep-ex]

60. ATLAS Collaboration, Calibration of b-tagging using dileptonic top pair events in a combinatorial likelihood approach with the ATLAS experiment. ATLAS-CONF-2014-004, 2014. http://cds.cern.ch/record/1664335

61. ATLAS Collaboration, Performance of missing transverse momentum reconstruction in proton–proton collisions at $\sqrt{s} = 7$ TeV with ATLAS. Eur. Phys. J. C **72**, 1844 (2012). doi:10.1140/epjc/s10052-011-1844-6. arXiv:1108.5602 [hep-ex]

62. ATLAS Collaboration, Selection of jets produced in proton–proton collisions with the ATLAS detector using 2011 data. ATLAS-CONF-2012-020, 2012. http://cds.cern.ch/record/1430034

63. J. Erdmann et al., A likelihood-based reconstruction algorithm for top-quark pairs and the KLFitter framework. Nucl. Instrum. Methods A **748**, 18 (2014). doi:10.1016/j.nima.2014.02.029. arXiv:1312.5595 [hep-ex]

64. ATLAS Collaboration, Measurements of spin correlation in top–antitop quark events from proton–proton collisions at $\sqrt{s} = 7$ TeV using the ATLAS detector. Phys. Rev. D **90**, 112016 (2014). doi:10.1103/PhysRevD.90.112016. arXiv:1407.4314 [hep-ex]

65. ATLAS Collaboration, Electron reconstruction and identification efficiency measurements with the ATLAS detector using the 2011 LHC proton–proton collision data. Eur. Phys. J. C **74**, 2941 (2014). doi:10.1140/epjc/s10052-014-2941-0. arXiv:1404.2240 [hep-ex]

66. ATLAS Collaboration, Muon reconstruction efficiency and momentum resolution of the ATLAS experiment in proton–proton collisions at $\sqrt{s} = 7$ TeV in 2010. Eur. Phys. J. C **74**, 3034 (2014). doi:10.1140/epjc/s10052-014-3034-9. arXiv:1404.4562 [hep-ex]

67. ATLAS Collaboration, Electron performance measurements with the ATLAS detector using the 2010 LHC proton–proton collision data. Eur. Phys. J. C **72**, 1909 (2012). doi:10.1140/epjc/s10052-012-1909-1. arXiv:1110.3174 [hep-ex]

68. ATLAS Collaboration, Measurement of the muon reconstruction performance of the ATLAS detector using 2011 and 2012 LHC proton–proton collision data. Eur. Phys. J. C **74**, 3130 (2014). doi:10.1140/epjc/s10052-014-3130-x. arXiv:1407.3935 [hep-ex]

69. ATLAS Collaboration, Electron and photon energy calibration with the ATLAS detector using LHC run 1 data. Eur. Phys. J. C **74**, 3071 (2014). doi:10.1140/epjc/s10052-014-3071-4. arXiv:1407.5063 [hep-ex]

70. ATLAS Collaboration, Jet energy resolution in proton–proton collisions at $\sqrt{s} = 7$ TeV recorded in 2010 with the ATLAS detector. Eur. Phys. J. C **73**, 2306 (2013). doi:10.1140/epjc/s10052-013-2306-0. arXiv:1210.6210 [hep-ex]

71. ATLAS Collaboration, Performance of pile-up mitigation techniques for jets in pp collisions at $\sqrt{s} = 8$ TeV using the ATLAS detector. Eur. Phys. J. C **76**, 581 (2016). doi:10.1140/epjc/s10052-016-4395-z. arXiv: 1510.03823 [hep-ex]

72. ATLAS Collaboration, Pile-up subtraction and suppression for jets in ATLAS. ATLAS-CONF-2013-083, 2013. http://cds.cern.ch/record/1570994

73. M. Botje et al., The PDF4LHC Working Group Interim Recommendations (2011). arXiv:1101.0538 [hep-ph]

74. R.D. Ball et al., Parton distributions with LHC data. Nucl. Phys. B **867**, 244 (2013). doi:10.1016/j.nuclphysb.2012.10.003. arXiv:1207.1303 [hep-ph]

75. ATLAS Collaboration, Luminosity determination in pp collisions at $\sqrt{s} = 8$ TeV using the ATLAS detector at the LHC. Eur. Phys. J. C **76**, 653 (2016). doi:10.1140/epjc/s10052-016-4466-1. arXiv:1608.03953 [hep-ex]

76. J.A. Aguilar-Saavedra, J. Carvalho, N.F. Castro, F. Veloso, A. Onofre, Probing anomalous Wtb couplings in top pair decays. Eur. Phys. J. C **50**, 519 (2007). doi:10.1140/epjc/s10052-007-0289-4. arXiv:hep-ph/0605190 [hep-ph]

77. N. Castro, J. Erdmann, C. Grunwald, K. Kröninger, N.-A. Rosien, EFTfitter–a tool for interpreting measurements in the context of effective field theories. Eur. Phys. J. C **76**, 432 (2016). doi:10.1140/epjc/s10052-016-4280-9. arXiv:1605.05585 [hep-ex]

78. ATLAS Collaboration, Search for anomalous couplings in the Wtb vertex from the measurement of double differential angular decay rates of single top quarks produced in the t-channel with the ATLAS detector. JHEP **04**, 023 (2016). doi:10.1007/JHEP04(2016)023. arXiv:1510.03764 [hep-ex]

79. CMS Collaboration, Measurement of the t-channel single-top-quark production cross section and of the $|V_{tb}|$ CKM matrix element in pp collisions at $\sqrt{s} = 8$ TeV. JHEP **06**, 090 (2014). doi:10.1007/JHEP06(2014)090. arXiv:1403.7366 [hep-ex]

80. ATLAS Collaboration, Comprehensive measurements of t-channel single top-quark production cross sections at $\sqrt{s} = 7$ TeV with the ATLAS detector. Phys. Rev. D **90**, 112006 (2014). doi:10.1103/PhysRevD.90.112006. arXiv:1406.7844 [hep-ex]

81. B. Grzadkowski, M. Misiak, Anomalous Wtb coupling effects in the weak radiative B-meson decay. Phys. Rev. D **78**, 077501 (2008). [Erratum: Phys. Rev. D **84**, 059903 (2011)]. doi:10.1103/PhysRevD.84.059903, doi:10.1103/PhysRevD.78.077501. arXiv:0802.1413 [hep-ph]

82. ATLAS Collaboration, ATLAS Computing Acknowledgements 2016–2017. ATL-GEN-PUB-2016-002, 2016. http://cds.cern.ch/record/2202407

ATLAS Collaboration

M. Aaboud[137d], G. Aad[88], B. Abbott[115], J. Abdallah[8], O. Abdinov[12], B. Abeloos[119], O. S. AbouZeid[139], N. L. Abraham[151], H. Abramowicz[155], H. Abreu[154], R. Abreu[118], Y. Abulaiti[148a,148b], B. S. Acharya[167a,167b,a], S. Adachi[157], L. Adamczyk[41a], D. L. Adams[27], J. Adelman[110], S. Adomeit[102], T. Adye[133], A. A. Affolder[139], T. Agatonovic-Jovin[14], J. A. Aguilar-Saavedra[128a,128f], S. P. Ahlen[24], F. Ahmadov[68,b], G. Aielli[135a,135b], H. Akerstedt[148a,148b], T. P. A. Åkesson[84], A. V. Akimov[98], G. L. Alberghi[22a,22b], J. Albert[172], S. Albrand[58], M. J. Alconada Verzini[74], M. Aleksa[32], I. N. Aleksandrov[68], C. Alexa[28b], G. Alexander[155], T. Alexopoulos[10], M. Alhroob[115], B. Ali[130], M. Aliev[76a,76b], G. Alimonti[94a], J. Alison[33], S. P. Alkire[38], B. M. M. Allbrooke[151], B. W. Allen[118], P. P. Allport[19], A. Aloisio[106a,106b], A. Alonso[39], F. Alonso[74], C. Alpigiani[140], A. A. Alshehri[56], M. Alstaty[88], B. Alvarez Gonzalez[32], D. Álvarez Piqueras[170], M. G. Alviggi[106a,106b], B. T. Amadio[16], Y. Amaral Coutinho[26a], C. Amelung[25], D. Amidei[92], S. P. Amor Dos Santos[128a,128c], A. Amorim[128a,128b], S. Amoroso[32], G. Amundsen[25], C. Anastopoulos[141], L. S. Ancu[52], N. Andari[19], T. Andeen[11], C. F. Anders[60b], J. K. Anders[77], K. J. Anderson[33], A. Andreazza[94a,94b], V. Andrei[60a], S. Angelidakis[9], I. Angelozzi[109], A. Angerami[38], F. Anghinolfi[32], A. V. Anisenkov[111,c], N. Anjos[13], A. Annovi[126a,126b], C. Antel[60a], M. Antonelli[50], A. Antonov[100,*], D. J. Antrim[166], F. Anulli[134a], M. Aoki[69], L. Aperio Bella[19], G. Arabidze[93], Y. Arai[69], J. P. Araque[128a], V. Araujo Ferraz[26a], A. T. H. Arce[48], F. A. Arduh[74], J-F. Arguin[97], S. Argyropoulos[66], M. Arik[20a], A. J. Armbruster[145], L. J. Armitage[79], O. Arnaez[32], H. Arnold[51], M. Arratia[30], O. Arslan[23], A. Artamonov[99], G. Artoni[122], S. Artz[86], S. Asai[157], N. Asbah[45], A. Ashkenazi[155], B. Åsman[148a,148b], L. Asquith[151], K. Assamagan[27], R. Astalos[146a], M. Atkinson[169], N. B. Atlay[143], K. Augsten[130], G. Avolio[32], B. Axen[16], M. K. Ayoub[119], G. Azuelos[97,d], M. A. Baak[32], A. E. Baas[60a], M. J. Baca[19], H. Bachacou[138], K. Bachas[76a,76b], M. Backes[122], M. Backhaus[32], P. Bagiacchi[134a,134b], P. Bagnaia[134a,134b], Y. Bai[35a], J. T. Baines[133], M. Bajic[39], O. K. Baker[179], E. M. Baldin[111,c], P. Balek[175], T. Balestri[150], F. Balli[138], W. K. Balunas[124], E. Banas[42], Sw. Banerjee[176,e], A. A. E. Bannoura[178], L. Barak[32], E. L. Barberio[91], D. Barberis[53a,53b], M. Barbero[88], T. Barillari[103], M-S. Barisits[32], T. Barklow[145], N. Barlow[30], S. L. Barnes[87], B. M. Barnett[133], R. M. Barnett[16], Z. Barnovska-Blenessy[36a], A. Baroncelli[136a], G. Barone[25], A. J. Barr[122],

L. Barranco Navarro[170], F. Barreiro[85], J. Barreiro Guimarães da Costa[35a], R. Bartoldus[145], A. E. Barton[75], P. Bartos[146a], A. Basalaev[125], A. Bassalat[119,f], R. L. Bates[56], S. J. Batista[161], J. R. Batley[30], M. Battaglia[139], M. Bauce[134a,134b], F. Bauer[138], H. S. Bawa[145,g], J. B. Beacham[113], M. D. Beattie[75], T. Beau[83], P. H. Beauchemin[165], P. Bechtle[23], H. P. Beck[18,h], K. Becker[122], M. Becker[86], M. Beckingham[173], C. Becot[112], A. J. Beddall[20d], A. Beddall[20b], V. A. Bednyakov[68], M. Bedognetti[109], C. P. Bee[150], L. J. Beemster[109], T. A. Beermann[32], M. Begel[27], J. K. Behr[45], A. S. Bell[81], G. Bella[155], L. Bellagamba[22a], A. Bellerive[31], M. Bellomo[89], K. Belotskiy[100], O. Beltramello[32], N. L. Belyaev[100], O. Benary[155,*], D. Benchekroun[137a], M. Bender[102], K. Bendtz[148a,148b], N. Benekos[10], Y. Benhammou[155], E. Benhar Noccioli[179], J. Benitez[66], D. P. Benjamin[48], J. R. Bensinger[25], S. Bentvelsen[109], L. Beresford[122], M. Beretta[50], D. Berge[109], E. Bergeaas Kuutmann[168], N. Berger[5], J. Beringer[16], S. Berlendis[58], N. R. Bernard[89], C. Bernius[112], F. U. Bernlochner[23], T. Berry[80], P. Berta[131], C. Bertella[86], G. Bertoli[148a,148b], F. Bertolucci[126a,126b], I. A. Bertram[75], C. Bertsche[45], D. Bertsche[115], G. J. Besjes[39], O. Bessidskaia Bylund[148a,148b], M. Bessner[45], N. Besson[138], C. Betancourt[51], A. Bethani[58], S. Bethke[103], A. J. Bevan[79], R. M. Bianchi[127], M. Bianco[32], O. Biebel[102], D. Biedermann[17], R. Bielski[87], N. V. Biesuz[126a,126b], M. Biglietti[136a], J. Bilbao De Mendizabal[52], T. R. V. Billoud[97], H. Bilokon[50], M. Bindi[57], A. Bingul[20b], C. Bini[134a,134b], S. Biondi[22a,22b], T. Bisanz[57], D. M. Bjergaard[48], C. W. Black[152], J. E. Black[145], K. M. Black[24], D. Blackburn[140], R. E. Blair[6], T. Blazek[146a], I. Bloch[45], C. Blocker[25], A. Blue[56], W. Blum[86,*], U. Blumenschein[57], S. Blunier[34a], G. J. Bobbink[109], V. S. Bobrovnikov[111,c], S. S. Bocchetta[84], A. Bocci[48], C. Bock[102], M. Boehler[51], D. Boerner[178], J. A. Bogaerts[32], D. Bogavac[102], A. G. Bogdanchikov[111], C. Bohm[148a], V. Boisvert[80], P. Bokan[14], T. Bold[41a], A. S. Boldyrev[101], M. Bomben[83], M. Bona[79], M. Boonekamp[138], A. Borisov[132], G. Borissov[75], J. Bortfeldt[32], D. Bortoletto[122], V. Bortolotto[62a,62b,62c], K. Bos[109], D. Boscherini[22a], M. Bosman[13], J. D. Bossio Sola[29], J. Boudreau[127], J. Bouffard[2], E. V. Bouhova-Thacker[75], D. Boumediene[37], C. Bourdarios[119], S. K. Boutle[56], A. Boveia[113], J. Boyd[32], I. R. Boyko[68], J. Bracinik[19], A. Brandt[8], G. Brandt[57], O. Brandt[60a], U. Bratzler[158], B. Brau[89], J. E. Brau[118], W. D. Breaden Madden[56], K. Brendlinger[124], A. J. Brennan[91], L. Brenner[109], R. Brenner[168], S. Bressler[175], T. M. Bristow[49], D. Britton[56], D. Britzger[45], F. M. Brochu[30], I. Brock[23], R. Brock[93], G. Brooijmans[38], T. Brooks[80], W. K. Brooks[34b], J. Brosamer[16], E. Brost[110], J. H Broughton[19], P. A. Bruckman de Renstrom[42], D. Bruncko[146b], R. Bruneliere[51], A. Bruni[22a], G. Bruni[22a], L. S. Bruni[109], BH. Brunt[30], M. Bruschi[22a], N. Bruscino[23], P. Bryant[33], L. Bryngemark[84], T. Buanes[15], Q. Buat[144], P. Buchholz[143], A. G. Buckley[56], I. A. Budagov[68], F. Buehrer[51], M. K. Bugge[121], O. Bulekov[100], D. Bullock[8], H. Burckhart[32], S. Burdin[77], C. D. Burgard[51], A. M. Burger[5], B. Burghgrave[110], K. Burka[42], S. Burke[133], I. Burmeister[46], J. T. P. Burr[122], E. Busato[37], D. Büscher[51], V. Büscher[86], P. Bussey[56], J. M. Butler[24], C. M. Buttar[56], J. M. Butterworth[81], P. Butti[109], W. Buttinger[27], A. Buzatu[56], A. R. Buzykaev[111,c], S. Cabrera Urbán[170], D. Caforio[130], V. M. Cairo[40a,40b], O. Cakir[4a], N. Calace[52], P. Calafiura[16], A. Calandri[88], G. Calderini[83], P. Calfayan[64], G. Callea[40a,40b], L. P. Caloba[26a], S. Calvente Lopez[85], D. Calvet[37], S. Calvet[37], T. P. Calvet[88], R. Camacho Toro[33], S. Camarda[32], P. Camarri[135a,135b], D. Cameron[121], R. Caminal Armadans[169], C. Camincher[58], S. Campana[32], M. Campanelli[81], A. Camplani[94a,94b], A. Campoverde[143], V. Canale[106a,106b], A. Canepa[163a], M. Cano Bret[36c], J. Cantero[116], T. Cao[155], M. D. M. Capeans Garrido[32], I. Caprini[28b], M. Caprini[28b], M. Capua[40a,40b], R. M. Carbone[38], R. Cardarelli[135a], F. Cardillo[51], I. Carli[131], T. Carli[32], G. Carlino[106a], B. T. Carlson[127], L. Carminati[94a,94b], R. M. D. Carney[148a,148b], S. Caron[108], E. Carquin[34b], G. D. Carrillo-Montoya[32], J. R. Carter[30], J. Carvalho[128a,128c], D. Casadei[19], M. P. Casado[13,i], M. Casolino[13], D. W. Casper[166], E. Castaneda-Miranda[147a], R. Castelijn[109], A. Castelli[109], V. Castillo Gimenez[170], N. F. Castro[128a,j], A. Catinaccio[32], J. R. Catmore[121], A. Cattai[32], J. Caudron[23], V. Cavaliere[169], E. Cavallaro[13], D. Cavalli[94a], M. Cavalli-Sforza[13], V. Cavasinni[126a,126b], F. Ceradini[136a,136b], L. Cerda Alberich[170], A. S. Cerqueira[26b], A. Cerri[151], L. Cerrito[135a,135b], F. Cerutti[16], A. Cervelli[18], S. A. Cetin[20c], A. Chafaq[137a], D. Chakraborty[110], S. K. Chan[59], Y. L. Chan[62a], P. Chang[169], J. D. Chapman[30], D. G. Charlton[19], A. Chatterjee[52], C. C. Chau[161], C. A. Chavez Barajas[151], S. Che[113], S. Cheatham[167a,167c], A. Chegwidden[93], S. Chekanov[6], S. V. Chekulaev[163a], G. A. Chelkov[68,k], M. A. Chelstowska[92], C. Chen[67], H. Chen[27], S. Chen[35b], S. Chen[157], X. Chen[35c], Y. Chen[70], H. C. Cheng[92], H. J Cheng[35a], Y. Cheng[33], A. Cheplakov[68], E. Cheremushkina[132], R. Cherkaoui El Moursli[137e], V. Chernyatin[27,*], E. Cheu[7], L. Chevalier[138], V. Chiarella[50], G. Chiarelli[126a,126b], G. Chiodini[76a], A. S. Chisholm[32], A. Chitan[28b], M. V. Chizhov[68], K. Choi[64], A. R. Chomont[37], S. Chouridou[9], B. K. B. Chow[102], V. Christodoulou[81], D. Chromek-Burckhart[32], J. Chudoba[129], A. J. Chuinard[90], J. J. Chwastowski[42], L. Chytka[117], A. K. Ciftci[4a], D. Cinca[46], V. Cindro[78], I. A. Cioara[23], C. Ciocca[22a,22b], A. Ciocio[16], F. Cirotto[106a,106b], Z. H. Citron[175], M. Citterio[94a], M. Ciubancan[28b], A. Clark[52], B. L. Clark[59], M. R. Clark[38], P. J. Clark[49], R. N. Clarke[16], C. Clement[148a,148b], Y. Coadou[88], M. Cobal[167a,167c], A. Coccaro[52], J. Cochran[67], L. Colasurdo[108], B. Cole[38], A. P. Colijn[109], J. Collot[58], T. Colombo[166], P. Conde Muiño[128a,128b], E. Coniavitis[51], S. H. Connell[147b], I. A. Connelly[80], V. Consorti[51], S. Constantinescu[28b], G. Conti[32], F. Conventi[106a,l], M. Cooke[16], B. D. Cooper[81], A. M. Cooper-Sarkar[122], F. Cormier[171], K. J. R. Cormier[161], T. Cornelissen[178], M. Corradi[134a,134b], F. Corriveau[90,m], A. Cortes-Gonzalez[32], G. Cortiana[103], G. Costa[94a],

M. J. Costa[170], D. Costanzo[141], G. Cottin[30], G. Cowan[80], B. E. Cox[87], K. Cranmer[112], S. J. Crawley[56], G. Cree[31], S. Crépé-Renaudin[58], F. Crescioli[83], W. A. Cribbs[148a,148b], M. Crispin Ortuzar[122], M. Cristinziani[23], V. Croft[108], G. Crosetti[40a,40b], A. Cueto[85], T. Cuhadar Donszelmann[141], J. Cummings[179], M. Curatolo[50], J. Cúth[86], H. Czirr[143], P. Czodrowski[3], G. D'amen[22a,22b], S. D'Auria[56], M. D'Onofrio[77], M. J. Da Cunha Sargedas De Sousa[128a,128b], C. Da Via[87], W. Dabrowski[41a], T. Dado[146a], T. Dai[92], O. Dale[15], F. Dallaire[97], C. Dallapiccola[89], M. Dam[39], J. R. Dandoy[33], N. P. Dang[51], A. C. Daniells[19], N. S. Dann[87], M. Danninger[171], M. Dano Hoffmann[138], V. Dao[51], G. Darbo[53a], S. Darmora[8], J. Dassoulas[3], A. Dattagupta[118], W. Davey[23], C. David[45], T. Davidek[131], M. Davies[155], P. Davison[81], E. Dawe[91], I. Dawson[141], K. De[8], R. de Asmundis[106a], A. De Benedetti[115], S. De Castro[22a,22b], S. De Cecco[83], N. De Groot[108], P. de Jong[109], H. De la Torre[93], F. De Lorenzi[67], A. De Maria[57], D. De Pedis[134a], A. De Salvo[134a], U. De Sanctis[151], A. De Santo[151], J. B. De Vivie De Regie[119], W. J. Dearnaley[75], R. Debbe[27], C. Debenedetti[139], D. V. Dedovich[68], N. Dehghanian[3], I. Deigaard[109], M. Del Gaudio[40a,40b], J. Del Peso[85], T. Del Prete[126a,126b], D. Delgove[119], F. Deliot[138], C. M. Delitzsch[52], A. Dell'Acqua[32], L. Dell'Asta[24], M. Dell'Orso[126a,126b], M. Della Pietra[106a,l], D. della Volpe[52], M. Delmastro[5], P. A. Delsart[58], D. A. DeMarco[161], S. Demers[179], M. Demichev[68], A. Demilly[83], S. P. Denisov[132], D. Denysiuk[138], D. Derendarz[42], J. E. Derkaoui[137d], F. Derue[83], P. Dervan[77], K. Desch[23], C. Deterre[45], K. Dette[46], P. O. Deviveiros[32], A. Dewhurst[133], S. Dhaliwal[25], A. Di Ciaccio[135a,135b], L. Di Ciaccio[5], W. K. Di Clemente[124], C. Di Donato[106a,106b], A. Di Girolamo[32], B. Di Girolamo[32], B. Di Micco[136a,136b], R. Di Nardo[32], K. F. Di Petrillo[59], A. Di Simone[51], R. Di Sipio[161], D. Di Valentino[31], C. Diaconu[88], M. Diamond[161], F. A. Dias[49], M. A. Diaz[34a], E. B. Diehl[92], J. Dietrich[17], S. Díez Cornell[45], A. Dimitrievska[14], J. Dingfelder[23], P. Dita[28b], S. Dita[28b], F. Dittus[32], F. Djama[88], T. Djobava[54b], J. I. Djuvsland[60a], M. A. B. do Vale[26c], D. Dobos[32], M. Dobre[28b], C. Doglioni[84], J. Dolejsi[131], Z. Dolezal[131], M. Donadelli[26d], S. Donati[126a,126b], P. Dondero[123a,123b], J. Donini[37], J. Dopke[133], A. Doria[106a], M. T. Dova[74], A. T. Doyle[56], E. Drechsler[57], M. Dris[10], Y. Du[36b], J. Duarte-Campderros[155], E. Duchovni[175], G. Duckeck[102], O. A. Ducu[97,n], D. Duda[109], A. Dudarev[32], A. Chr. Dudder[86], E. M. Duffield[16], L. Duflot[119], M. Dührssen[32], M. Dumancic[175], A. K. Duncan[56], M. Dunford[60a], H. Duran Yildiz[4a], M. Düren[55], A. Durglishvili[54b], D. Duschinger[47], B. Dutta[45], M. Dyndal[45], C. Eckardt[45], K. M. Ecker[103], R. C. Edgar[92], N. C. Edwards[49], T. Eifert[32], G. Eigen[15], K. Einsweiler[16], T. Ekelof[168], M. El Kacimi[137c], V. Ellajosyula[88], M. Ellert[168], S. Elles[5], F. Ellinghaus[178], A. A. Elliot[172], N. Ellis[32], J. Elmsheuser[27], M. Elsing[32], D. Emeliyanov[133], Y. Enari[157], O. C. Endner[86], J. S. Ennis[173], J. Erdmann[46], A. Ereditato[18], G. Ernis[178], J. Ernst[2], M. Ernst[27], S. Errede[169], E. Ertel[86], M. Escalier[119], H. Esch[46], C. Escobar[127], B. Esposito[50], A. I. Etienvre[138], E. Etzion[155], H. Evans[64], A. Ezhilov[125], M. Ezzi[137e], F. Fabbri[22a,22b], L. Fabbri[22a,22b], G. Facini[33], R. M. Fakhrutdinov[132], S. Falciano[134a], R. J. Falla[81], J. Faltova[32], Y. Fang[35a], M. Fanti[94a,94b], A. Farbin[8], A. Farilla[136a], C. Farina[127], E. M. Farina[123a,123b], T. Farooque[13], S. Farrell[16], S. M. Farrington[173], P. Farthouat[32], F. Fassi[137e], P. Fassnacht[32], D. Fassouliotis[9], M. Faucci Giannelli[80], A. Favareto[53a,53b], W. J. Fawcett[122], L. Fayard[119], O. L. Fedin[125,o], W. Fedorko[171], S. Feigl[121], L. Feligioni[88], C. Feng[36b], E. J. Feng[32], H. Feng[92], A. B. Fenyuk[132], L. Feremenga[8], P. Fernandez Martinez[170], S. Fernandez Perez[13], J. Ferrando[45], A. Ferrari[168], P. Ferrari[109], R. Ferrari[123a], D. E. Ferreira de Lima[60b], A. Ferrer[170], D. Ferrere[52], C. Ferretti[92], F. Fiedler[86], A. Filipčič[78], M. Filipuzzi[45], F. Filthaut[108], M. Fincke-Keeler[172], K. D. Finelli[152], M. C. N. Fiolhais[128a,128c], L. Fiorini[170], A. Fischer[2], C. Fischer[13], J. Fischer[178], W. C. Fisher[93], N. Flaschel[45], I. Fleck[143], P. Fleischmann[92], G. T. Fletcher[141], R. R. M. Fletcher[124], T. Flick[178], B. M. Flierl[102], L. R. Flores Castillo[62a], M. J. Flowerdew[103], G. T. Forcolin[87], A. Formica[138], A. Forti[87], A. G. Foster[19], D. Fournier[119], H. Fox[75], S. Fracchia[13], P. Francavilla[83], M. Franchini[22a,22b], D. Francis[32], L. Franconi[121], M. Franklin[59], M. Frate[166], M. Fraternali[123a,123b], D. Freeborn[81], S. M. Fressard-Batraneanu[32], F. Friedrich[47], D. Froidevaux[32], J. A. Frost[122], C. Fukunaga[158], E. Fullana Torregrosa[86], T. Fusayasu[104], J. Fuster[170], C. Gabaldon[58], O. Gabizon[154], A. Gabrielli[22a,22b], A. Gabrielli[16], G. P. Gach[41a], S. Gadatsch[32], G. Gagliardi[53a,53b], L. G. Gagnon[97], P. Gagnon[64], C. Galea[108], B. Galhardo[128a,128c], E. J. Gallas[122], B. J. Gallop[133], P. Gallus[130], G. Galster[39], K. K. Gan[113], S. Ganguly[37], J. Gao[36a], Y. Gao[49], Y. S. Gao[145,g], F. M. Garay Walls[49], C. García[170], J. E. García Navarro[170], M. Garcia-Sciveres[16], R. W. Gardner[33], N. Garelli[145], V. Garonne[121], A. Gascon Bravo[45], K. Gasnikova[45], C. Gatti[50], A. Gaudiello[53a,53b], G. Gaudio[123a], L. Gauthier[97], I. L. Gavrilenko[98], C. Gay[171], G. Gaycken[23], E. N. Gazis[10], Z. Gecse[171], C. N. P. Gee[133], Ch. Geich-Gimbel[23], M. Geisen[86], M. P. Geisler[60a], K. Gellerstedt[148a,148b], C. Gemme[53a], M. H. Genest[58], C. Geng[36a,p], S. Gentile[134a,134b], C. Gentsos[156], S. George[80], D. Gerbaudo[13], A. Gershon[155], S. Ghasemi[143], M. Ghneimat[23], B. Giacobbe[22a], S. Giagu[134a,134b], P. Giannetti[126a,126b], S. M. Gibson[80], M. Gignac[171], M. Gilchriese[16], T. P. S. Gillam[30], D. Gillberg[31], G. Gilles[178], D. M. Gingrich[3,d], N. Giokaris[9,*], M. P. Giordani[167a,167c], F. M. Giorgi[22a], P. F. Giraud[138], P. Giromini[59], D. Giugni[94a], F. Giuli[122], C. Giuliani[103], M. Giulini[60b], B. K. Gjelsten[121], S. Gkaitatzis[156], I. Gkialas[156], E. L. Gkougkousis[139], L. K. Gladilin[101], C. Glasman[85], J. Glatzer[13], P. C. F. Glaysher[49], A. Glazov[45], M. Goblirsch-Kolb[25], J. Godlewski[42], S. Goldfarb[91], T. Golling[52], D. Golubkov[132], A. Gomes[128a,128b,128d], R. Gonçalo[128a], R. Goncalves Gama[26a], J. Goncalves Pinto Firmino Da Costa[138], G. Gonella[51], L. Gonella[19],

A. Gongadze[68], S. González de la Hoz[170], S. Gonzalez-Sevilla[52], L. Goossens[32], P. A. Gorbounov[99], H. A. Gordon[27], I. Gorelov[107], B. Gorini[32], E. Gorini[76a,76b], A. Gorišek[78], A. T. Goshaw[48], C. Gössling[46], M. I. Gostkin[68], C. R. Goudet[119], D. Goujdami[137c], A. G. Goussiou[140], N. Govender[147b,q], E. Gozani[154], L. Graber[57], I. Grabowska-Bold[41a], P. O. J. Gradin[58], P. Grafström[22a,22b], J. Gramling[52], E. Gramstad[121], S. Grancagnolo[17], V. Gratchev[125], P. M. Gravila[28e], H. M. Gray[32], E. Graziani[136a], Z. D. Greenwood[82,r], C. Grefe[23], K. Gregersen[81], I. M. Gregor[45], P. Grenier[145], K. Grevtsov[5], J. Griffiths[8], A. A. Grillo[139], K. Grimm[75], S. Grinstein[13,s], Ph. Gris[37], J. -F. Grivaz[119], S. Groh[86], E. Gross[175], J. Grosse-Knetter[57], G. C. Grossi[82], Z. J. Grout[81], L. Guan[92], W. Guan[176], J. Guenther[65], F. Guescini[52], D. Guest[166], O. Gueta[155], B. Gui[113], E. Guido[53a,53b], T. Guillemin[5], S. Guindon[2], U. Gul[56], C. Gumpert[32], J. Guo[36c], W. Guo[92], Y. Guo[36a,p], R. Gupta[43], S. Gupta[122], G. Gustavino[134a,134b], P. Gutierrez[115], N. G. Gutierrez Ortiz[81], C. Gutschow[81], C. Guyot[138], C. Gwenlan[122], C. B. Gwilliam[77], A. Haas[112], C. Haber[16], H. K. Hadavand[8], N. Haddad[137e], A. Hadef[88], S. Hageböck[23], M. Hagihara[164], H. Hakobyan[180,*], M. Haleem[45], J. Haley[116], G. Halladjian[93], G. D. Hallewell[88], K. Hamacher[178], P. Hamal[117], K. Hamano[172], A. Hamilton[147a], G. N. Hamity[141], P. G. Hamnett[45], L. Han[36a], S. Han[35a], K. Hanagaki[69,t], K. Hanawa[157], M. Hance[139], B. Haney[124], P. Hanke[60a], R. Hanna[138], J. B. Hansen[39], J. D. Hansen[39], M. C. Hansen[23], P. H. Hansen[39], K. Hara[164], A. S. Hard[176], T. Harenberg[178], F. Hariri[119], S. Harkusha[95], R. D. Harrington[49], P. F. Harrison[173], F. Hartjes[109], N. M. Hartmann[102], M. Hasegawa[70], Y. Hasegawa[142], A. Hasib[115], S. Hassani[138], S. Haug[18], R. Hauser[93], L. Hauswald[47], M. Havranek[129], C. M. Hawkes[19], R. J. Hawkings[32], D. Hayakawa[159], D. Hayden[93], C. P. Hays[122], J. M. Hays[79], H. S. Hayward[77], S. J. Haywood[133], S. J. Head[19], T. Heck[86], V. Hedberg[84], L. Heelan[8], S. Heim[124], T. Heim[16], B. Heinemann[45], J. J. Heinrich[102], L. Heinrich[112], C. Heinz[55], J. Hejbal[129], L. Helary[32], S. Hellman[148a,148b], C. Helsens[32], J. Henderson[122], R. C. W. Henderson[75], Y. Heng[176], S. Henkelmann[171], A. M. Henriques Correia[32], S. Henrot-Versille[119], G. H. Herbert[17], H. Herde[25], V. Herget[177], Y. Hernández Jiménez[147c], G. Herten[51], R. Hertenberger[102], L. Hervas[32], G. G. Hesketh[81], N. P. Hessey[109], J. W. Hetherly[43], E. Higón-Rodriguez[170], E. Hill[172], J. C. Hill[30], K. H. Hiller[45], S. J. Hillier[19], I. Hinchliffe[16], E. Hines[124], M. Hirose[51], D. Hirschbuehl[178], O. Hladik[129], X. Hoad[49], J. Hobbs[150], N. Hod[163a], M. C. Hodgkinson[141], P. Hodgson[141], A. Hoecker[32], M. R. Hoeferkamp[107], F. Hoenig[102], D. Hohn[23], T. R. Holmes[16], M. Homann[46], S. Honda[164], T. Honda[69], T. M. Hong[127], B. H. Hooberman[169], W. H. Hopkins[118], Y. Horii[105], A. J. Horton[144], J-Y. Hostachy[58], S. Hou[153], A. Hoummada[137a], J. Howarth[45], J. Hoya[74], M. Hrabovsky[117], I. Hristova[17], J. Hrivnac[119], T. Hryn'ova[5], A. Hrynevich[96], P. J. Hsu[63], S. -C. Hsu[140], Q. Hu[36a], S. Hu[36c], Y. Huang[45], Z. Hubacek[130], F. Hubaut[88], F. Huegging[23], T. B. Huffman[122], E. W. Hughes[38], G. Hughes[75], M. Huhtinen[32], P. Huo[150], N. Huseynov[68,b], J. Huston[93], J. Huth[59], G. Iacobucci[52], G. Iakovidis[27], I. Ibragimov[143], L. Iconomidou-Fayard[119], E. Ideal[179], Z. Idrissi[137e], P. Iengo[32], O. Igonkina[109,u], T. Iizawa[174], Y. Ikegami[69], M. Ikeno[69], Y. Ilchenko[11,v], D. Iliadis[156], N. Ilic[145], G. Introzzi[123a,123b], P. Ioannou[9,*], M. Iodice[136a], K. Iordanidou[38], V. Ippolito[59], N. Ishijima[120], M. Ishino[157], M. Ishitsuka[159], C. Issever[122], S. Istin[20a], F. Ito[164], J. M. Iturbe Ponce[87], R. Iuppa[162a,162b], H. Iwasaki[69], J. M. Izen[44], V. Izzo[106a], S. Jabbar[3], B. Jackson[124], P. Jackson[1], V. Jain[2], K. B. Jakobi[86], K. Jakobs[51], S. Jakobsen[32], T. Jakoubek[129], D. O. Jamin[116], D. K. Jana[82], R. Jansky[65], J. Janssen[23], M. Janus[57], P. A. Janus[41a], G. Jarlskog[84], N. Javadov[68,b], T. Javůrek[51], F. Jeanneau[138], L. Jeanty[16], J. Jejelava[54a,w], G.-Y. Jeng[152], P. Jenni[51,x], C. Jeske[173], S. Jézéquel[5], H. Ji[176], J. Jia[150], H. Jiang[67], Y. Jiang[36a], Z. Jiang[145], S. Jiggins[81], J. Jimenez Pena[170], S. Jin[35a], A. Jinaru[28b], O. Jinnouchi[159], H. Jivan[147c], P. Johansson[141], K. A. Johns[7], C. A. Johnson[64], W. J. Johnson[140], K. Jon-And[148a,148b], G. Jones[173], R. W. L. Jones[75], S. Jones[7], T. J. Jones[77], J. Jongmanns[60a], P. M. Jorge[128a,128b], J. Jovicevic[163a], X. Ju[176], A. Juste Rozas[13,s], M. K. Köhler[175], A. Kaczmarska[42], M. Kado[119], H. Kagan[113], M. Kagan[145], S. J. Kahn[88], T. Kaji[174], E. Kajomovitz[48], C. W. Kalderon[122], A. Kaluza[86], S. Kama[43], A. Kamenshchikov[132], N. Kanaya[157], S. Kaneti[30], L. Kanjir[78], V. A. Kantserov[100], J. Kanzaki[69], B. Kaplan[112], L. S. Kaplan[176], A. Kapliy[33], D. Kar[147c], K. Karakostas[10], A. Karamaoun[3], N. Karastathis[10], M. J. Kareem[57], E. Karentzos[10], S. N. Karpov[68], Z. M. Karpova[68], K. Karthik[112], V. Kartvelishvili[75], A. N. Karyukhin[132], K. Kasahara[164], L. Kashif[176], R. D. Kass[113], A. Kastanas[149], Y. Kataoka[157], C. Kato[157], A. Katre[52], J. Katzy[45], K. Kawade[105], K. Kawagoe[73], T. Kawamoto[157], G. Kawamura[57], V. F. Kazanin[111,c], R. Keeler[172], R. Kehoe[43], J. S. Keller[45], J. J. Kempster[80], H. Keoshkerian[161], O. Kepka[129], B. P. Kerševan[78], S. Kersten[178], R. A. Keyes[90], M. Khader[169], F. Khalil-zada[12], A. Khanov[116], A. G. Kharlamov[111,c], T. Kharlamova[111], T. J. Khoo[52], V. Khovanskiy[99], E. Khramov[68], J. Khubua[54b,y], S. Kido[70], C. R. Kilby[80], H. Y. Kim[8], S. H. Kim[164], Y. K. Kim[33], N. Kimura[156], O. M. Kind[17], B. T. King[77], M. King[170], J. Kirk[133], A. E. Kiryunin[103], T. Kishimoto[157], D. Kisielewska[41a], F. Kiss[51], K. Kiuchi[164], O. Kivernyk[138], E. Kladiva[146b], T. Klapdor-kleingrothaus[51], M. H. Klein[38], M. Klein[77], U. Klein[77], K. Kleinknecht[86], P. Klimek[110], A. Klimentov[27], R. Klingenberg[46], T. Klioutchnikova[32], E.-E. Kluge[60a], P. Kluit[109], S. Kluth[103], J. Knapik[42], E. Kneringer[65], E. B. F. G. Knoops[88], A. Knue[103], A. Kobayashi[157], D. Kobayashi[159], T. Kobayashi[157], M. Kobel[47], M. Kocian[145], P. Kodys[131], T. Koffas[31], E. Koffeman[109], N. M. Köhler[103], T. Koi[145], H. Kolanoski[17], M. Kolb[60b], I. Koletsou[5], A. A. Komar[98,*], Y. Komori[157], T. Kondo[69], N. Kondrashova[36c], K. Köneke[51], A. C. König[108], T. Kono[69,z], R. Konoplich[112,aa], N. Konstantinidis[81], R. Kopeliansky[64], S. Koperny[41a],

A. K. Kopp[51], K. Korcyl[42], K. Kordas[156], A. Korn[81], A. A. Korol[111,c], I. Korolkov[13], E. V. Korolkova[141], O. Kortner[103], S. Kortner[103], T. Kosek[131], V. V. Kostyukhin[23], A. Kotwal[48], A. Koulouris[10], A. Kourkoumeli-Charalampidi[123a,123b], C. Kourkoumelis[9], V. Kouskoura[27], A. B. Kowalewska[42], R. Kowalewski[172], T. Z. Kowalski[41a], C. Kozakai[157], W. Kozanecki[138], A. S. Kozhin[132], V. A. Kramarenko[101], G. Kramberger[78], D. Krasnopevtsev[100], M. W. Krasny[83], A. Krasznahorkay[32], A. Kravchenko[27], M. Kretz[60c], J. Kretzschmar[77], K. Kreutzfeldt[55], P. Krieger[161], K. Krizka[33], K. Kroeninger[46], H. Kroha[103], J. Kroll[124], J. Kroseberg[23], J. Krstic[14], U. Kruchonak[68], H. Krüger[23], N. Krumnack[67], M. C. Kruse[48], M. Kruskal[24], T. Kubota[91], H. Kucuk[81], S. Kuday[4b], J. T. Kuechler[178], S. Kuehn[51], A. Kugel[60c], F. Kuger[177], T. Kuhl[45], V. Kukhtin[68], R. Kukla[138], Y. Kulchitsky[95], S. Kuleshov[34b], M. Kuna[134a,134b], T. Kunigo[71], A. Kupco[129], O. Kuprash[155], H. Kurashige[70], L. L. Kurchaninov[163a], Y. A. Kurochkin[95], M. G. Kurth[44], V. Kus[129], E. S. Kuwertz[172], M. Kuze[159], J. Kvita[117], T. Kwan[172], D. Kyriazopoulos[141], A. La Rosa[103], J. L. La Rosa Navarro[26d], L. La Rotonda[40a,40b], C. Lacasta[170], F. Lacava[134a,134b], J. Lacey[31], H. Lacker[17], D. Lacour[83], E. Ladygin[68], R. Lafaye[5], B. Laforge[83], T. Lagouri[179], S. Lai[57], S. Lammers[64], W. Lampl[7], E. Lançon[138], U. Landgraf[51], M. P. J. Landon[79], M. C. Lanfermann[52], V. S. Lang[60a], J. C. Lange[13], A. J. Lankford[166], F. Lanni[27], K. Lantzsch[23], A. Lanza[123a], S. Laplace[83], C. Lapoire[32], J. F. Laporte[138], T. Lari[94a], F. Lasagni Manghi[22a,22b], M. Lassnig[32], P. Laurelli[50], W. Lavrijsen[16], A. T. Law[139], P. Laycock[77], T. Lazovich[59], M. Lazzaroni[94a,94b], B. Le[91], O. Le Dortz[83], E. Le Guirriec[88], E. P. Le Quilleuc[138], M. LeBlanc[172], T. LeCompte[6], F. Ledroit-Guillon[58], C. A. Lee[27], S. C. Lee[153], L. Lee[1], B. Lefebvre[90], G. Lefebvre[83], M. Lefebvre[172], F. Legger[102], C. Leggett[16], A. Lehan[77], G. Lehmann Miotto[32], X. Lei[7], W. A. Leight[31], A. G. Leister[179], M. A. L. Leite[26d], R. Leitner[131], D. Lellouch[175], B. Lemmer[57], K. J. C. Leney[81], T. Lenz[23], B. Lenzi[32], R. Leone[7], S. Leone[126a,126b], C. Leonidopoulos[49], S. Leontsinis[10], G. Lerner[151], C. Leroy[97], A. A. J. Lesage[138], C. G. Lester[30], M. Levchenko[125], J. Levêque[5], D. Levin[92], L. J. Levinson[175], M. Levy[19], D. Lewis[79], M. Leyton[44], B. Li[36a,p], C. Li[36a], H. Li[150], L. Li[48], L. Li[36c], Q. Li[35a], S. Li[48], X. Li[87], Y. Li[143], Z. Liang[35a], B. Liberti[135a], A. Liblong[161], P. Lichard[32], K. Lie[169], J. Liebal[23], W. Liebig[15], A. Limosani[152], S. C. Lin[153,ab], T. H. Lin[86], B. E. Lindquist[150], A. E. Lionti[52], E. Lipeles[124], A. Lipniacka[15], M. Lisovyi[60b], T. M. Liss[169], A. Lister[171], A. M. Litke[139], B. Liu[153,ac], D. Liu[153], H. Liu[92], H. Liu[27], J. Liu[36b], J. B. Liu[36a], K. Liu[88], L. Liu[169], M. Liu[36a], Y. L. Liu[36a], Y. Liu[36a], M. Livan[123a,123b], A. Lleres[58], J. Llorente Merino[35a], S. L. Lloyd[79], F. Lo Sterzo[153], E. M. Lobodzinska[45], P. Loch[7], F. K. Loebinger[87], K. M. Loew[25], A. Loginov[179,*], T. Lohse[17], K. Lohwasser[45], M. Lokajicek[129], B. A. Long[24], J. D. Long[169], R. E. Long[75], L. Longo[76a,76b], K. A. Looper[113], J. A. Lopez Lopez[34b], D. Lopez Mateos[59], B. Lopez Paredes[141], I. Lopez Paz[13], A. Lopez Solis[83], J. Lorenz[102], N. Lorenzo Martinez[64], M. Losada[21], P. J. Lösel[102], X. Lou[35a], A. Lounis[119], J. Love[6], P. A. Love[75], H. Lu[62a], N. Lu[92], H. J. Lubatti[140], C. Luci[134a,134b], A. Lucotte[58], C. Luedtke[51], F. Luehring[64], W. Lukas[65], L. Luminari[134a], O. Lundberg[148a,148b], B. Lund-Jensen[149], P. M. Luzi[83], D. Lynn[27], R. Lysak[129], E. Lytken[84], V. Lyubushkin[68], H. Ma[27], L. L. Ma[36b], Y. Ma[36b], G. Maccarrone[50], A. Macchiolo[103], C. M. Macdonald[141], B. Maček[78], J. Machado Miguens[124,128b], D. Madaffari[88], R. Madar[37], H. J. Maddocks[168], W. F. Mader[47], A. Madsen[45], J. Maeda[70], S. Maeland[15], T. Maeno[27], A. Maevskiy[101], E. Magradze[57], J. Mahlstedt[109], C. Maiani[119], C. Maidantchik[26a], A. A. Maier[103], T. Maier[102], A. Maio[128a,128b,128d], S. Majewski[118], Y. Makida[69], N. Makovec[119], B. Malaescu[83], Pa. Malecki[42], V. P. Maleev[125], F. Malek[58], U. Mallik[66], D. Malon[6], C. Malone[30], S. Maltezos[10], S. Malyukov[32], J. Mamuzic[170], G. Mancini[50], L. Mandelli[94a], I. Mandić[78], J. Maneira[128a,128b], L. Manhaes de Andrade Filho[26b], J. Manjarres Ramos[163b], A. Mann[102], A. Manousos[32], B. Mansoulie[138], J. D. Mansour[35a], R. Mantifel[90], M. Mantoani[57], S. Manzoni[94a,94b], L. Mapelli[32], G. Marceca[29], L. March[52], G. Marchiori[83], M. Marcisovsky[129], M. Marjanovic[14], D. E. Marley[92], F. Marroquim[26a], S. P. Marsden[87], gnmZ. Marshall[16], S. Marti-Garcia[170], B. Martin[93], T. A. Martin[173], V. J. Martin[49], B. Martin dit Latour[15], M. Martinez[13,s], V. I. Martinez Outschoorn[169], S. Martin-Haugh[133], V. S. Martoiu[28b], A. C. Martyniuk[81], A. Marzin[32], L. Masetti[86], T. Mashimo[157], R. Mashinistov[98], J. Masik[87], A. L. Maslennikov[111,c], I. Massa[22a,22b], L. Massa[22a,22b], P. Mastrandrea[5], A. Mastroberardino[40a,40b], T. Masubuchi[157], P. Mättig[178], J. Mattmann[86], J. Maurer[28b], S. J. Maxfield[77], D. A. Maximov[111,c], R. Mazini[153], I. Maznas[156], S. M. Mazza[94a,94b], N. C. Mc Fadden[107], G. Mc Goldrick[161], S. P. Mc Kee[92], A. McCarn[92], R. L. McCarthy[150], T. G. McCarthy[103], L. I. McClymont[81], E. F. McDonald[91], J. A. Mcfayden[81], G. Mchedlidze[57], S. J. McMahon[133], R. A. McPherson[172,m], M. Medinnis[45], S. Meehan[140], S. Mehlhase[102], A. Mehta[77], K. Meier[60a], C. Meineck[102], B. Meirose[44], D. Melini[170], B. R. Mellado Garcia[147c], M. Melo[146a], F. Meloni[18], S. B. Menary[87], L. Meng[77], X. T. Meng[92], A. Mengarelli[22a,22b], S. Menke[103], E. Meoni[165], S. Mergelmeyer[17], P. Mermod[52], L. Merola[106a,106b], C. Meroni[94a], F. S. Merritt[33], A. Messina[134a,134b], J. Metcalfe[6], A. S. Mete[166], C. Meyer[86], C. Meyer[124], J-P. Meyer[138], J. Meyer[109], H. Meyer Zu Theenhausen[60a], F. Miano[151], R. P. Middleton[133], S. Miglioranzi[53a,53b], L. Mijović[49], G. Mikenberg[175], M. Mikestikova[129], M. Mikuž[78], M. Milesi[91], A. Milic[27], D. W. Miller[33], C. Mills[49], A. Milov[175], D. A. Milstead[148a,148b], A. A. Minaenko[132], Y. Minami[157], I. A. Minashvili[68], A. I. Mincer[112], B. Mindur[41a], M. Mineev[68], Y. Minegishi[157], Y. Ming[176], L. M. Mir[13], K. P. Mistry[124], T. Mitani[174], J. Mitrevski[102], V. A. Mitsou[170], A. Miucci[18], P. S. Miyagawa[141],

A. Mizukami[69], J. U. Mjörnmark[84], M. Mlynarikova[131], T. Moa[148a,148b], K. Mochizuki[97], P. Mogg[51], S. Mohapatra[38], S. Molander[148a,148b], R. Moles-Valls[23], R. Monden[71], M. C. Mondragon[93], K. Mönig[45], J. Monk[39], E. Monnier[88], A. Montalbano[150], J. Montejo Berlingen[32], F. Monticelli[74], S. Monzani[94a,94b], R. W. Moore[3], N. Morange[119], D. Moreno[21], M. Moreno Llácer[57], P. Morettini[53a], S. Morgenstern[32], D. Mori[144], T. Mori[157], M. Morii[59], M. Morinaga[157], V. Morisbak[121], S. Moritz[86], A. K. Morley[152], G. Mornacchi[32], J. D. Morris[79], S. S. Mortensen[39], L. Morvaj[150], P. Moschovakos[10], M. Mosidze[54b], H. J. Moss[141], J. Moss[145,ad], K. Motohashi[159], R. Mount[145], E. Mountricha[27], E. J. W. Moyse[89], S. Muanza[88], R. D. Mudd[19], F. Mueller[103], J. Mueller[127], R. S. P. Mueller[102], T. Mueller[30], D. Muenstermann[75], P. Mullen[56], G. A. Mullier[18], F. J. Munoz Sanchez[87], J. A. Murillo Quijada[19], W. J. Murray[173,133], H. Musheghyan[57], M. Muškinja[78], A. G. Myagkov[132,ae], M. Myska[130], B. P. Nachman[16], O. Nackenhorst[52], K. Nagai[122], R. Nagai[69,z], K. Nagano[69], Y. Nagasaka[61], K. Nagata[164], M. Nagel[51], E. Nagy[88], A. M. Nairz[32], Y. Nakahama[105], K. Nakamura[69], T. Nakamura[157], I. Nakano[114], R. F. Naranjo Garcia[45], R. Narayan[11], D. I. Narrias Villar[60a], I. Naryshkin[125], T. Naumann[45], G. Navarro[21], R. Nayyar[7], H. A. Neal[92], P. Yu. Nechaeva[98], T. J. Neep[87], A. Negri[123a,123b], M. Negrini[22a], S. Nektarijevic[108], C. Nellist[119], A. Nelson[166], S. Nemecek[129], P. Nemethy[112], A. A. Nepomuceno[26a], M. Nessi[32,af], M. S. Neubauer[169], M. Neumann[178], R. M. Neves[112], P. Nevski[27], P. R. Newman[19], T. Nguyen Manh[97], R. B. Nickerson[122], R. Nicolaidou[138], J. Nielsen[139], V. Nikolaenko[132,ae], I. Nikolic-Audit[83], K. Nikolopoulos[19], J. K. Nilsen[121], P. Nilsson[27], Y. Ninomiya[157], A. Nisati[134a], R. Nisius[103], T. Nobe[157], M. Nomachi[120], I. Nomidis[31], T. Nooney[79], S. Norberg[115], M. Nordberg[32], N. Norjoharuddeen[122], O. Novgorodova[47], S. Nowak[103], M. Nozaki[69], L. Nozka[117], K. Ntekas[166], E. Nurse[81], F. Nuti[91], D. C. O'Neil[144], A. A. O'Rourke[45], V. O'Shea[56], F. G. Oakham[31,d], H. Oberlack[103], T. Obermann[23], J. Ocariz[83], A. Ochi[70], I. Ochoa[38], J. P. Ochoa-Ricoux[34a], S. Oda[73], S. Odaka[69], H. Ogren[64], A. Oh[87], S. H. Oh[48], C. C. Ohm[16], H. Ohman[168], H. Oide[53a,53b], H. Okawa[164], Y. Okumura[157], T. Okuyama[69], A. Olariu[28b], L. F. Oleiro Seabra[128a], S. A. Olivares Pino[49], D. Oliveira Damazio[27], A. Olszewski[42], J. Olszowska[42], A. Onofre[128a,128e], K. Onogi[105], P. U. E. Onyisi[11,v], M. J. Oreglia[33], Y. Oren[155], D. Orestano[136a,136b], N. Orlando[62b], R. S. Orr[161], B. Osculati[53a,53b,*], R. Ospanov[87], G. Otero y Garzon[29], H. Otono[73], M. Ouchrif[137d], F. Ould-Saada[121], A. Ouraou[138], K. P. Oussoren[109], Q. Ouyang[35a], M. Owen[56], R. E. Owen[19], V. E. Ozcan[20a], N. Ozturk[8], K. Pachal[144], A. Pacheco Pages[13], L. Pacheco Rodriguez[138], C. Padilla Aranda[13], M. Pagáčová[51], S. Pagan Griso[16], M. Paganini[179], F. Paige[27], P. Pais[89], K. Pajchel[121], G. Palacino[64], S. Palazzo[40a,40b], S. Palestini[32], M. Palka[41b], D. Pallin[37], E. St. Panagiotopoulou[10], C. E. Pandini[83], J. G. Panduro Vazquez[80], P. Pani[148a,148b], S. Panitkin[27], D. Pantea[28b], L. Paolozzi[52], Th. D. Papadopoulou[10], K. Papageorgiou[156], A. Paramonov[6], D. Paredes Hernandez[179], A. J. Parker[75], M. A. Parker[30], K. A. Parker[141], F. Parodi[53a,53b], J. A. Parsons[38], U. Parzefall[51], V. R. Pascuzzi[161], E. Pasqualucci[134a], S. Passaggio[53a], Fr. Pastore[80], G. Pásztor[31,ag], S. Pataraia[178], J. R. Pater[87], T. Pauly[32], J. Pearce[172], B. Pearson[115], L. E. Pedersen[39], M. Pedersen[121], S. Pedraza Lopez[170], R. Pedro[128a,128b], S. V. Peleganchuk[111,c], O. Penc[129], C. Peng[35a], H. Peng[36a], J. Penwell[64], B. S. Peralva[26b], M. M. Perego[138], D. V. Perepelitsa[27], E. Perez Codina[163a], L. Perini[94a,94b], H. Pernegger[32], S. Perrella[106a,106b], R. Peschke[45], V. D. Peshekhonov[68], K. Peters[45], R. F. Y. Peters[87], B. A. Petersen[32], T. C. Petersen[39], E. Petit[58], A. Petridis[1], C. Petridou[156], P. Petroff[119], E. Petrolo[134a], M. Petrov[122], F. Petrucci[136a,136b], N. E. Pettersson[89], A. Peyaud[138], R. Pezoa[34b], P. W. Phillips[133], G. Piacquadio[150], E. Pianori[173], A. Picazio[89], E. Piccaro[79], M. Piccinini[22a,22b], M. A. Pickering[122], R. Piegaia[29], J. E. Pilcher[33], A. D. Pilkington[87], A. W. J. Pin[87], M. Pinamonti[167a,167c,ah], J. L. Pinfold[3], A. Pingel[39], S. Pires[83], H. Pirumov[45], M. Pitt[175], L. Plazak[146a], M.-A. Pleier[27], V. Pleskot[86], E. Plotnikova[68], D. Pluth[67], R. Poettgen[148a,148b], L. Poggioli[119], D. Pohl[23], G. Polesello[123a], A. Poley[45], A. Policicchio[40a,40b], R. Polifka[161], A. Polini[22a], C. S. Pollard[56], V. Polychronakos[27], K. Pommès[32], L. Pontecorvo[134a], B. G. Pope[93], G. A. Popeneciu[28c], A. Poppleton[32], S. Pospisil[130], K. Potamianos[16], I. N. Potrap[68], C. J. Potter[30], C. T. Potter[118], G. Poulard[32], J. Poveda[32], V. Pozdnyakov[68], M. E. Pozo Astigarraga[32], P. Pralavorio[88], A. Pranko[16], S. Prell[67], D. Price[87], L. E. Price[6], M. Primavera[76a], S. Prince[90], K. Prokofiev[62c], F. Prokoshin[34b], S. Protopopescu[27], J. Proudfoot[6], M. Przybycien[41a], D. Puddu[136a,136b], M. Purohit[27,ai], P. Puzo[119], J. Qian[92], G. Qin[56], Y. Qin[87], A. Quadt[57], W. B. Quayle[167a,167b], M. Queitsch-Maitland[45], D. Quilty[56], S. Raddum[121], V. Radeka[27], V. Radescu[122], S. K. Radhakrishnan[150], P. Radloff[118], P. Rados[91], F. Ragusa[94a,94b], G. Rahal[181], J. A. Raine[87], S. Rajagopalan[27], M. Rammensee[32], C. Rangel-Smith[168], M. G. Ratti[94a,94b], D. M. Rauch[45], F. Rauscher[102], S. Rave[86], T. Ravenscroft[56], I. Ravinovich[175], M. Raymond[32], A. L. Read[121], N. P. Readioff[77], M. Reale[76a,76b], D. M. Rebuzzi[123a,123b], A. Redelbach[177], G. Redlinger[27], R. Reece[139], R. G. Reed[147c], K. Reeves[44], L. Rehnisch[17], J. Reichert[124], A. Reiss[86], C. Rembser[32], H. Ren[35a], M. Rescigno[134a], S. Resconi[94a], E. D. Resseguie[124], O. L. Rezanova[111,c], P. Reznicek[131], R. Rezvani[97], R. Richter[103], S. Richter[81], E. Richter-Was[41b], O. Ricken[23], M. Ridel[83], P. Rieck[103], C. J. Riegel[178], J. Rieger[57], O. Rifki[115], M. Rijssenbeek[150], A. Rimoldi[123a,123b], M. Rimoldi[18], L. Rinaldi[22a], B. Ristić[52], E. Ritsch[32], I. Riu[13], F. Rizatdinova[116], E. Rizvi[79], C. Rizzi[13], R. T. Roberts[87], S. H. Robertson[90,m], A. Robichaud-Veronneau[90], D. Robinson[30], J. E. M. Robinson[45], A. Robson[56], C. Roda[126a,126b], Y. Rodina[88,aj],

A. Rodriguez Perez[13], D. Rodriguez Rodriguez[170], S. Roe[32], C. S. Rogan[59], O. Røhne[121], J. Roloff[59], A. Romaniouk[100], M. Romano[22a,22b], S. M. Romano Saez[37], E. Romero Adam[170], N. Rompotis[140], M. Ronzani[51], L. Roos[83], E. Ros[170], S. Rosati[134a], K. Rosbach[51], P. Rose[139], N.-A. Rosien[57], V. Rossetti[148a,148b], E. Rossi[106a,106b], L. P. Rossi[53a], J. H. N. Rosten[30], R. Rosten[140], M. Rotaru[28b], I. Roth[175], J. Rothberg[140], D. Rousseau[119], A. Rozanov[88], Y. Rozen[154], X. Ruan[147c], F. Rubbo[145], M. S. Rudolph[161], F. Rühr[51], A. Ruiz-Martinez[31], Z. Rurikova[51], N. A. Rusakovich[68], A. Ruschke[102], H. L. Russell[140], J. P. Rutherfoord[7], N. Ruthmann[32], Y. F. Ryabov[125], M. Rybar[169], G. Rybkin[119], S. Ryu[6], A. Ryzhov[132], G. F. Rzehorz[57], A. F. Saavedra[152], G. Sabato[109], S. Sacerdoti[29], H. F-W. Sadrozinski[139], R. Sadykov[68], F. Safai Tehrani[134a], P. Saha[110], M. Sahinsoy[60a], M. Saimpert[138], T. Saito[157], H. Sakamoto[157], Y. Sakurai[174], G. Salamanna[136a,136b], A. Salamon[135a,135b], J. E. Salazar Loyola[34b], D. Salek[109], P. H. Sales De Bruin[140], D. Salihagic[103], A. Salnikov[145], J. Salt[170], D. Salvatore[40a,40b], F. Salvatore[151], A. Salvucci[62a,62b,62c], A. Salzburger[32], D. Sammel[51], D. Sampsonidis[156], J. Sánchez[170], V. Sanchez Martinez[170], A. Sanchez Pineda[106a,106b], H. Sandaker[121], R. L. Sandbach[79], M. Sandhoff[178], C. Sandoval[21], D. P. C. Sankey[133], M. Sannino[53a,53b], A. Sansoni[50], C. Santoni[37], R. Santonico[135a,135b], H. Santos[128a], I. Santoyo Castillo[151], K. Sapp[127], A. Sapronov[68], J. G. Saraiva[128a,128d], B. Sarrazin[23], O. Sasaki[69], K. Sato[164], E. Sauvan[5], G. Savage[80], P. Savard[161,d], N. Savic[103], C. Sawyer[133], L. Sawyer[82,r], J. Saxon[33], C. Sbarra[22a], A. Sbrizzi[22a,22b], T. Scanlon[81], D. A. Scannicchio[166], M. Scarcella[152], V. Scarfone[40a,40b], J. Schaarschmidt[175], P. Schacht[103], B. M. Schachtner[102], D. Schaefer[32], L. Schaefer[124], R. Schaefer[45], J. Schaeffer[86], S. Schaepe[23], S. Schaetzel[60b], U. Schäfer[86], A. C. Schaffer[119], D. Schaile[102], R. D. Schamberger[150], V. Scharf[60a], V. A. Schegelsky[125], D. Scheirich[131], M. Schernau[166], C. Schiavi[53a,53b], S. Schier[139], C. Schillo[51], M. Schioppa[40a,40b], S. Schlenker[32], K. R. Schmidt-Sommerfeld[103], K. Schmieden[32], C. Schmitt[86], S. Schmitt[45], S. Schmitz[86], B. Schneider[163a], U. Schnoor[51], L. Schoeffel[138], A. Schoening[60b], B. D. Schoenrock[93], E. Schopf[23], M. Schott[86], J. F. P. Schouwenberg[108], J. Schovancova[8], S. Schramm[52], M. Schreyer[177], N. Schuh[86], A. Schulte[86], M. J. Schultens[23], H.-C. Schultz-Coulon[60a], H. Schulz[17], M. Schumacher[51], B. A. Schumm[139], Ph. Schune[138], A. Schwartzman[145], T. A. Schwarz[92], H. Schweiger[87], Ph. Schwemling[138], R. Schwienhorst[93], J. Schwindling[138], T. Schwindt[23], G. Sciolla[25], F. Scuri[126a,126b], F. Scutti[91], J. Searcy[92], P. Seema[23], S. C. Seidel[107], A. Seiden[139], F. Seifert[130], J. M. Seixas[26a], G. Sekhniaidze[106a], K. Sekhon[92], S. J. Sekula[43], N. Semprini-Cesari[22a,22b], C. Serfon[121], L. Serin[119], L. Serkin[167a,167b], M. Sessa[136a,136b], R. Seuster[172], H. Severini[115], T. Sfiligoj[78], F. Sforza[32], A. Sfyrla[52], E. Shabalina[57], N. W. Shaikh[148a,148b], L. Y. Shan[35a], R. Shang[169], J. T. Shank[24], M. Shapiro[16], P. B. Shatalov[99], K. Shaw[167a,167b], S. M. Shaw[87], A. Shcherbakova[148a,148b], C. Y. Shehu[151], P. Sherwood[81], L. Shi[153,ak], S. Shimizu[70], C. O. Shimmin[166], M. Shimojima[104], S. Shirabe[73], M. Shiyakova[68,al], A. Shmeleva[98], D. Shoaleh Saadi[97], M. J. Shochet[33], S. Shojaii[94a], D. R. Shope[115], S. Shrestha[113], E. Shulga[100], M. A. Shupe[7], P. Sicho[129], A. M. Sickles[169], P. E. Sidebo[149], E. Sideras Haddad[147c], O. Sidiropoulou[177], D. Sidorov[116], A. Sidoti[22a,22b], F. Siegert[47], Dj. Sijacki[14], J. Silva[128a,128d], S. B. Silverstein[148a], V. Simak[130], Lj. Simic[14], S. Simion[119], E. Simioni[86], B. Simmons[81], D. Simon[37], M. Simon[86], P. Sinervo[161], N. B. Sinev[118], M. Sioli[22a,22b], G. Siragusa[177], I. Siral[92], S. Yu. Sivoklokov[101], J. Sjölin[148a,148b], M. B. Skinner[75], H. P. Skottowe[59], P. Skubic[115], M. Slater[19], T. Slavicek[130], M. Slawinska[109], K. Sliwa[165], R. Slovak[131], V. Smakhtin[175], B. H. Smart[5], L. Smestad[15], J. Smiesko[146a], S. Yu. Smirnov[100], Y. Smirnov[100], L. N. Smirnova[101,am], O. Smirnova[84], J. W. Smith[57], M. N. K. Smith[38], R. W. Smith[38], M. Smizanska[75], K. Smolek[130], A. A. Snesarev[98], I. M. Snyder[118], S. Snyder[27], R. Sobie[172,m], F. Socher[47], A. Soffer[155], D. A. Soh[153], G. Sokhrannyi[78], C. A. Solans Sanchez[32], M. Solar[130], E. Yu. Soldatov[100], U. Soldevila[170], A. A. Solodkov[132], A. Soloshenko[68], O. V. Solovyanov[132], V. Solovyev[125], P. Sommer[51], H. Son[165], H. Y. Song[36a,an], A. Sood[16], A. Sopczak[130], V. Sopko[130], V. Sorin[13], D. Sosa[60b], C. L. Sotiropoulou[126a,126b], R. Soualah[167a,167c], A. M. Soukharev[111,c], D. South[45], B. C. Sowden[80], S. Spagnolo[76a,76b], M. Spalla[126a,126b], M. Spangenberg[173], F. Spanò[80], D. Sperlich[17], F. Spettel[103], R. Spighi[22a], G. Spigo[32], L. A. Spiller[91], M. Spousta[131], R. D. St. Denis[56,*], A. Stabile[94a], R. Stamen[60a], S. Stamm[17], E. Stanecka[42], R. W. Stanek[6], C. Stanescu[136a], M. Stanescu-Bellu[45], M. M. Stanitzki[45], S. Stapnes[121], E. A. Starchenko[132], G. H. Stark[33], J. Stark[58], P. Staroba[129], P. Starovoitov[60a], S. Stärz[32], R. Staszewski[42], P. Steinberg[27], B. Stelzer[144], H. J. Stelzer[32], O. Stelzer-Chilton[163a], H. Stenzel[55], G. A. Stewart[56], J. A. Stillings[23], M. C. Stockton[90], M. Stoebe[90], G. Stoicea[28b], P. Stolte[57], S. Stonjek[103], A. R. Stradling[8], A. Straessner[47], M. E. Stramaglia[18], J. Strandberg[149], S. Strandberg[148a,148b], A. Strandlie[121], M. Strauss[115], P. Strizenec[146b], R. Ströhmer[177], D. M. Strom[118], R. Stroynowski[43], A. Strubig[108], S. A. Stucci[27], B. Stugu[15], N. A. Styles[45], D. Su[145], J. Su[127], S. Suchek[60a], Y. Sugaya[120], M. Suk[130], V. V. Sulin[98], S. Sultansoy[4c], T. Sumida[71], S. Sun[59], X. Sun[3], J. E. Sundermann[51], K. Suruliz[151], C. J. E. Suster[152], M. R. Sutton[151], S. Suzuki[69], M. Svatos[129], M. Swiatlowski[33], S. P. Swift[2], I. Sykora[146a], T. Sykora[131], D. Ta[51], K. Tackmann[45], J. Taenzer[155], A. Taffard[166], R. Tafirout[163a], N. Taiblum[155], H. Takai[27], R. Takashima[72], T. Takeshita[142], Y. Takubo[69], M. Talby[88], A. A. Talyshev[111,c], J. Tanaka[157], M. Tanaka[159], R. Tanaka[119], S. Tanaka[69], R. Tanioka[70], B. B. Tannenwald[113], S. Tapia Araya[34b], S. Tapprogge[86], S. Tarem[154], G. F. Tartarelli[94a], P. Tas[131], M. Tasevsky[129], T. Tashiro[71], E. Tassi[40a,40b], A. Tavares Delgado[128a,128b], Y. Tayalati[137e], A. C. Taylor[107],

G. N. Taylor[91], P. T. E. Taylor[91], W. Taylor[163b], F. A. Teischinger[32], P. Teixeira-Dias[80], K. K. Temming[51], D. Temple[144], H. Ten Kate[32], P. K. Teng[153], J. J. Teoh[120], F. Tepel[178], S. Terada[69], K. Terashi[157], J. Terron[85], S. Terzo[13], M. Testa[50], R. J. Teuscher[161,m], T. Theveneaux-Pelzer[88], J. P. Thomas[19], J. Thomas-Wilsker[80], P. D. Thompson[19], A. S. Thompson[56], L. A. Thomsen[179], E. Thomson[124], M. J. Tibbetts[16], R. E. Ticse Torres[88], V. O. Tikhomirov[98,ao], Yu. A. Tikhonov[111,c], S. Timoshenko[100], P. Tipton[179], S. Tisserant[88], K. Todome[159], T. Todorov[5,*], S. Todorova-Nova[131], J. Tojo[73], S. Tokár[146a], K. Tokushuku[69], E. Tolley[59], L. Tomlinson[87], M. Tomoto[105], L. Tompkins[145,ap], K. Toms[107], B. Tong[59], P. Tornambe[51], E. Torrence[118], H. Torres[144], E. Torró Pastor[140], J. Toth[88,aq], F. Touchard[88], D. R. Tovey[141], T. Trefzger[177], A. Tricoli[27], I. M. Trigger[163a], S. Trincaz-Duvoid[83], M. F. Tripiana[13], W. Trischuk[161], B. Trocmé[58], A. Trofymov[45], C. Troncon[94a], M. Trottier-McDonald[16], M. Trovatelli[172], L. Truong[167a,167c], M. Trzebinski[42], A. Trzupek[42], J. C-L. Tseng[122], P. V. Tsiareshka[95], G. Tsipolitis[10], N. Tsirintanis[9], S. Tsiskaridze[13], V. Tsiskaridze[51], E. G. Tskhadadze[54a], K. M. Tsui[62a], I. I. Tsukerman[99], V. Tsulaia[16], S. Tsuno[69], D. Tsybychev[150], Y. Tu[62b], A. Tudorache[28b], V. Tudorache[28b], T. T. Tulbure[28a], A. N. Tuna[59], S. A. Tupputi[22a,22b], S. Turchikhin[68], D. Turgeman[175], I. Turk Cakir[4b,ar], R. Turra[94a,94b], P. M. Tuts[38], G. Ucchielli[22a,22b], I. Ueda[157], M. Ughetto[148a,148b], F. Ukegawa[164], G. Unal[32], A. Undrus[27], G. Unel[166], F. C. Ungaro[91], Y. Unno[69], C. Unverdorben[102], J. Urban[146b], P. Urquijo[91], P. Urrejola[86], G. Usai[8], J. Usui[69], L. Vacavant[88], V. Vacek[130], B. Vachon[90], C. Valderanis[102], E. Valdes Santurio[148a,148b], N. Valencic[109], S. Valentinetti[22a,22b], A. Valero[170], L. Valery[13], S. Valkar[131], J. A. Valls Ferrer[170], W. Van Den Wollenberg[109], P. C. Van Der Deijl[109], H. van der Graaf[109], N. van Eldik[154], P. van Gemmeren[6], J. Van Nieuwkoop[144], I. van Vulpen[109], M. C. van Woerden[109], M. Vanadia[134a,134b], W. Vandelli[32], R. Vanguri[124], A. Vaniachine[160], P. Vankov[109], G. Vardanyan[180], R. Vari[134a], E. W. Varnes[7], T. Varol[43], D. Varouchas[83], A. Vartapetian[8], K. E. Varvell[152], J. G. Vasquez[179], G. A. Vasquez[34b], F. Vazeille[37], T. Vazquez Schroeder[90], J. Veatch[57], V. Veeraraghavan[7], L. M. Veloce[161], F. Veloso[128a,128c], S. Veneziano[134a], A. Ventura[76a,76b], M. Venturi[172], N. Venturi[161], A. Venturini[25], V. Vercesi[123a], M. Verducci[134a,134b], W. Verkerke[109], J. C. Vermeulen[109], A. Vest[47,as], M. C. Vetterli[144,d], O. Viazlo[84], I. Vichou[169,*], T. Vickey[141], O. E. Vickey Boeriu[141], G. H. A. Viehhauser[122], S. Viel[16], L. Vigani[122], M. Villa[22a,22b], M. Villaplana Perez[94a,94b], E. Vilucchi[50], M. G. Vincter[31], V. B. Vinogradov[68], A. Vishwakarma[45], C. Vittori[22a,22b], I. Vivarelli[151], S. Vlachos[10], M. Vlasak[130], M. Vogel[178], P. Vokac[130], G. Volpi[126a,126b], M. Volpi[91], H. von der Schmitt[103], E. von Toerne[23], V. Vorobel[131], K. Vorobev[100], M. Vos[170], R. Voss[32], J. H. Vossebeld[77], N. Vranjes[14], M. Vranjes Milosavljevic[14], V. Vrba[129], M. Vreeswijk[109], R. Vuillermet[32], I. Vukotic[33], P. Wagner[23], W. Wagner[178], H. Wahlberg[74], S. Wahrmund[47], J. Wakabayashi[105], J. Walder[75], R. Walker[102], W. Walkowiak[143], V. Wallangen[148a,148b], C. Wang[35b], C. Wang[36b,88], F. Wang[176], H. Wang[16], H. Wang[43], J. Wang[45], J. Wang[152], K. Wang[90], Q. Wang[115], R. Wang[6], S. M. Wang[153], T. Wang[38], W. Wang[36a], C. Wanotayaroj[118], A. Warburton[90], C. P. Ward[30], D. R. Wardrope[81], A. Washbrook[49], P. M. Watkins[19], A. T. Watson[19], M. F. Watson[19], G. Watts[140], S. Watts[87], B. M. Waugh[81], S. Webb[86], M. S. Weber[18], S. W. Weber[177], S. A. Weber[31], J. S. Webster[6], A. R. Weidberg[122], B. Weinert[64], J. Weingarten[57], C. Weiser[51], H. Weits[109], P. S. Wells[32], T. Wenaus[27], T. Wengler[32], S. Wenig[32], N. Wermes[23], M. D. Werner[67], P. Werner[32], M. Wessels[60a], J. Wetter[165], K. Whalen[118], N. L. Whallon[140], A. M. Wharton[75], A. White[8], M. J. White[1], R. White[34b], D. Whiteson[166], F. J. Wickens[133], W. Wiedenmann[176], M. Wielers[133], C. Wiglesworth[39], L. A. M. Wiik-Fuchs[23], A. Wildauer[103], F. Wilk[87], H. G. Wilkens[32], H. H. Williams[124], S. Williams[109], C. Willis[93], S. Willocq[89], J. A. Wilson[19], I. Wingerter-Seez[5], F. Winklmeier[118], O. J. Winston[151], B. T. Winter[23], M. Wittgen[145], M. Wobisch[82,r], T. M. H. Wolf[109], R. Wolff[88], M. W. Wolter[42], H. Wolters[128a,128c], S. D. Worm[133], B. K. Wosiek[42], J. Wotschack[32], M. J. Woudstra[87], K. W. Wozniak[42], M. Wu[58], M. Wu[33], S. L. Wu[176], X. Wu[52], Y. Wu[92], T. R. Wyatt[87], B. M. Wynne[49], S. Xella[39], Z. Xi[92], D. Xu[35a], L. Xu[27], B. Yabsley[152], S. Yacoob[147a], D. Yamaguchi[159], Y. Yamaguchi[120], A. Yamamoto[69], S. Yamamoto[157], T. Yamanaka[157], K. Yamauchi[105], Y. Yamazaki[70], Z. Yan[24], H. Yang[36c], H. Yang[176], Y. Yang[153], Z. Yang[15], W-M. Yao[16], Y. C. Yap[83], Y. Yasu[69], E. Yatsenko[5], K. H. Yau Wong[23], J. Ye[43], S. Ye[27], I. Yeletskikh[68], E. Yildirim[86], K. Yorita[174], R. Yoshida[6], K. Yoshihara[124], C. Young[145], C. J. S. Young[32], S. Youssef[24], D. R. Yu[16], J. Yu[8], J. M. Yu[92], J. Yu[67], L. Yuan[70], S. P. Y. Yuen[23], I. Yusuff[30,at], B. Zabinski[42], R. Zaidan[66], A. M. Zaitsev[132,ae], N. Zakharchuk[45], J. Zalieckas[15], A. Zaman[150], S. Zambito[59], D. Zanzi[91], C. Zeitnitz[178], M. Zeman[130], A. Zemla[41a], J. C. Zeng[169], Q. Zeng[145], O. Zenin[132], T. Ženiš[146a], D. Zerwas[119], D. Zhang[92], F. Zhang[176], G. Zhang[36a,an], H. Zhang[35b], J. Zhang[6], L. Zhang[51], L. Zhang[36a], M. Zhang[169], R. Zhang[23], R. Zhang[36a,au], X. Zhang[36b], Z. Zhang[119], X. Zhao[43], Y. Zhao[36b], Z. Zhao[36a], A. Zhemchugov[68], J. Zhong[122], B. Zhou[92], C. Zhou[176], L. Zhou[38], L. Zhou[43], M. Zhou[35a], M. Zhou[150], N. Zhou[35c], C. G. Zhu[36b], H. Zhu[35a], J. Zhu[92], Y. Zhu[36a], X. Zhuang[35a], K. Zhukov[98], A. Zibell[177], D. Zieminska[64], N. I. Zimine[68], C. Zimmermann[86], S. Zimmermann[51], Z. Zinonos[57], M. Zinser[86], M. Ziolkowski[143], L. Živković[14], G. Zobernig[176], A. Zoccoli[22a,22b], M. zur Nedden[17], L. Zwalinski[32]

[1] Department of Physics, University of Adelaide, Adelaide, Australia

[2] Physics Department, SUNY Albany, Albany, NY, USA

[3] Department of Physics, University of Alberta, Edmonton, AB, Canada

[4] [a]Department of Physics, Ankara University, Ankara, Turkey; [b]Istanbul Aydin University, Istanbul, Turkey; [c]Division of Physics, TOBB University of Economics and Technology, Ankara, Turkey

[5] LAPP, CNRS/IN2P3 and Université Savoie Mont Blanc, Annecy-le-Vieux, France

[6] High Energy Physics Division, Argonne National Laboratory, Argonne, IL, USA

[7] Department of Physics, University of Arizona, Tucson, AZ, USA

[8] Department of Physics, The University of Texas at Arlington, Arlington, TX, USA

[9] Physics Department, National and Kapodistrian University of Athens, Athens, Greece

[10] Physics Department, National Technical University of Athens, Zografou, Greece

[11] Department of Physics, The University of Texas at Austin, Austin, TX, USA

[12] Institute of Physics, Azerbaijan Academy of Sciences, Baku, Azerbaijan

[13] Institut de Física d'Altes Energies (IFAE), The Barcelona Institute of Science and Technology, Barcelona, Spain

[14] Institute of Physics, University of Belgrade, Belgrade, Serbia

[15] Department for Physics and Technology, University of Bergen, Bergen, Norway

[16] Physics Division, Lawrence Berkeley National Laboratory and University of California, Berkeley, CA, USA

[17] Department of Physics, Humboldt University, Berlin, Germany

[18] Albert Einstein Center for Fundamental Physics and Laboratory for High Energy Physics, University of Bern, Bern, Switzerland

[19] School of Physics and Astronomy, University of Birmingham, Birmingham, UK

[20] [a]Department of Physics, Bogazici University, Istanbul, Turkey; [b]Department of Physics Engineering, Gaziantep University, Gaziantep, Turkey; [c]Faculty of Engineering and Natural Sciences, Istanbul Bilgi University, Istanbul, Turkey; [d]Faculty of Engineering and Natural Sciences, Bahcesehir University, Istanbul, Turkey

[21] Centro de Investigaciones, Universidad Antonio Narino, Bogota, Colombia

[22] [a]INFN Sezione di Bologna, Bologna, Italy; [b]Dipartimento di Fisica e Astronomia, Università di Bologna, Bologna, Italy

[23] Physikalisches Institut, University of Bonn, Bonn, Germany

[24] Department of Physics, Boston University, Boston, MA, USA

[25] Department of Physics, Brandeis University, Waltham, MA, USA

[26] [a]Universidade Federal do Rio De Janeiro COPPE/EE/IF, Rio de Janeiro, Brazil; [b]Electrical Circuits Department, Federal University of Juiz de Fora (UFJF), Juiz de Fora, Brazil; [c]Federal University of Sao Joao del Rei (UFSJ), São João del Rei, Brazil; [d]Instituto de Fisica, Universidade de Sao Paulo, São Paulo, Brazil

[27] Physics Department, Brookhaven National Laboratory, Upton, NY, USA

[28] [a]Transilvania University of Brasov, Brasov, Romania; [b]National Institute of Physics and Nuclear Engineering, Bucharest, Romania; [c]Physics Department, National Institute for Research and Development of Isotopic and Molecular Technologies, Cluj-Napoca, Romania; [d]University Politehnica Bucharest, Bucharest, Romania; [e]West University in Timisoara, Timisoara, Romania

[29] Departamento de Física, Universidad de Buenos Aires, Buenos Aires, Argentina

[30] Cavendish Laboratory, University of Cambridge, Cambridge, UK

[31] Department of Physics, Carleton University, Ottawa, ON, Canada

[32] CERN, Geneva, Switzerland

[33] Enrico Fermi Institute, University of Chicago, Chicago, IL, USA

[34] [a]Departamento de Física, Pontificia Universidad Católica de Chile, Santiago, Chile; [b]Departamento de Física, Universidad Técnica Federico Santa María, Valparaíso, Chile

[35] [a]Institute of High Energy Physics, Chinese Academy of Sciences, Beijing, China; [b]Department of Physics, Nanjing University, Jiangsu, China; [c]Physics Department, Tsinghua University, Beijing 100084, China

[36] [a]Department of Modern Physics, University of Science and Technology of China, Anhui, China; [b]School of Physics, Shandong University, Shandong, China; [c]Department of Physics and Astronomy, Shanghai Key Laboratory for Particle Physics and Cosmology, Shanghai Jiao Tong University (also affiliated with PKU-CHEP), Shanghai, China

[37] Laboratoire de Physique Corpusculaire, Université Clermont Auvergne, Université Blaise Pascal, CNRS/IN2P3, Clermont-Ferrand, France

[38] Nevis Laboratory, Columbia University, Irvington, NY, USA

[39] Niels Bohr Institute, University of Copenhagen, Copenhagen, Denmark

[40] (a)INFN Gruppo Collegato di Cosenza, Laboratori Nazionali di Frascati, Frascati, Italy; (b)Dipartimento di Fisica, Università della Calabria, Rende, Italy

[41] (a)Faculty of Physics and Applied Computer Science, AGH University of Science and Technology, Kraków, Poland ; (b)Marian Smoluchowski Institute of Physics, Jagiellonian University, Kraków, Poland

[42] Institute of Nuclear Physics, Polish Academy of Sciences, Kraków, Poland

[43] Physics Department, Southern Methodist University, Dallas, TX, USA

[44] Physics Department, University of Texas at Dallas, Richardson, TX, USA

[45] DESY, Hamburg and Zeuthen, Germany

[46] Lehrstuhl für Experimentelle Physik IV, Technische Universität Dortmund, Dortmund, Germany

[47] Institut für Kern- und Teilchenphysik, Technische Universität Dresden, Dresden, Germany

[48] Department of Physics, Duke University, Durham, NC, USA

[49] SUPA-School of Physics and Astronomy, University of Edinburgh, Edinburgh, UK

[50] INFN Laboratori Nazionali di Frascati, Frascati, Italy

[51] Fakultät für Mathematik und Physik, Albert-Ludwigs-Universität, Freiburg, Germany

[52] Departement de Physique Nucleaire et Corpusculaire, Université de Genève, Geneva, Switzerland

[53] (a)INFN Sezione di Genova, Genoa, Italy; (b)Dipartimento di Fisica, Università di Genova, Genoa, Italy

[54] (a)E. Andronikashvili Institute of Physics, Iv. Javakhishvili Tbilisi State University, Tbilisi, Georgia; (b)High Energy Physics Institute, Tbilisi State University, Tbilisi, Georgia

[55] II Physikalisches Institut, Justus-Liebig-Universität Giessen, Giessen, Germany

[56] SUPA-School of Physics and Astronomy, University of Glasgow, Glasgow, UK

[57] II Physikalisches Institut, Georg-August-Universität, Göttingen, Germany

[58] Laboratoire de Physique Subatomique et de Cosmologie, Université Grenoble-Alpes, CNRS/IN2P3, Grenoble, France

[59] Laboratory for Particle Physics and Cosmology, Harvard University, Cambridge, MA, USA

[60] (a)Kirchhoff-Institut für Physik, Ruprecht-Karls-Universität Heidelberg, Heidelberg, Germany; (b)Physikalisches Institut, Ruprecht-Karls-Universität Heidelberg, Heidelberg, Germany; (c)ZITI Institut für technische Informatik, Ruprecht-Karls-Universität Heidelberg, Mannheim, Germany

[61] Faculty of Applied Information Science, Hiroshima Institute of Technology, Hiroshima, Japan

[62] (a)Department of Physics, The Chinese University of Hong Kong, Shatin, N.T., Hong Kong; (b)Department of Physics, The University of Hong Kong, Hong Kong, China; (c)Department of Physics and Institute for Advanced Study, The Hong Kong University of Science and Technology, Clear Water Bay, Kowloon, Hong Kong, China

[63] Department of Physics, National Tsing Hua University, Hsinchu, Taiwan

[64] Department of Physics, Indiana University, Bloomington, IN, USA

[65] Institut für Astro- und Teilchenphysik, Leopold-Franzens-Universität, Innsbruck, Austria

[66] University of Iowa, Iowa City, IA, USA

[67] Department of Physics and Astronomy, Iowa State University, Ames, IA, USA

[68] Joint Institute for Nuclear Research, JINR Dubna, Dubna, Russia

[69] KEK, High Energy Accelerator Research Organization, Tsukuba, Japan

[70] Graduate School of Science, Kobe University, Kobe, Japan

[71] Faculty of Science, Kyoto University, Kyoto, Japan

[72] Kyoto University of Education, Kyoto, Japan

[73] Department of Physics, Kyushu University, Fukuoka, Japan

[74] Instituto de Física La Plata, Universidad Nacional de La Plata and CONICET, La Plata, Argentina

[75] Physics Department, Lancaster University, Lancaster, UK

[76] (a)INFN Sezione di Lecce, Lecce, Italy; (b)Dipartimento di Matematica e Fisica, Università del Salento, Lecce, Italy

[77] Oliver Lodge Laboratory, University of Liverpool, Liverpool, UK

[78] Department of Experimental Particle Physics, Jožef Stefan Institute and Department of Physics, University of Ljubljana, Ljubljana, Slovenia

[79] School of Physics and Astronomy, Queen Mary University of London, London, UK

[80] Department of Physics, Royal Holloway University of London, Surrey, UK

[81] Department of Physics and Astronomy, University College London, London, UK

[82] Louisiana Tech University, Ruston, LA, USA

[83] Laboratoire de Physique Nucléaire et de Hautes Energies, UPMC and Université Paris-Diderot and CNRS/IN2P3, Paris, France

[84] Fysiska institutionen, Lunds universitet, Lund, Sweden

[85] Departamento de Fisica Teorica C-15, Universidad Autonoma de Madrid, Madrid, Spain

[86] Institut für Physik, Universität Mainz, Mainz, Germany

[87] School of Physics and Astronomy, University of Manchester, Manchester, UK

[88] CPPM, Aix-Marseille Université and CNRS/IN2P3, Marseille, France

[89] Department of Physics, University of Massachusetts, Amherst, MA, USA

[90] Department of Physics, McGill University, Montreal, QC, Canada

[91] School of Physics, University of Melbourne, Melbourne, VIC, Australia

[92] Department of Physics, The University of Michigan, Ann Arbor, MI, USA

[93] Department of Physics and Astronomy, Michigan State University, East Lansing, MI, USA

[94] [a]INFN Sezione di Milano, Milan, Italy; [b]Dipartimento di Fisica, Università di Milano, Milan, Italy

[95] B.I. Stepanov Institute of Physics, National Academy of Sciences of Belarus, Minsk, Republic of Belarus

[96] Research Institute for Nuclear Problems of Byelorussian State University, Minsk, Republic of Belarus

[97] Group of Particle Physics, University of Montreal, Montreal, QC, Canada

[98] P.N. Lebedev Physical Institute of the Russian Academy of Sciences, Moscow, Russia

[99] Institute for Theoretical and Experimental Physics (ITEP), Moscow, Russia

[100] National Research Nuclear University MEPhI, Moscow, Russia

[101] D.V. Skobeltsyn Institute of Nuclear Physics, M.V. Lomonosov Moscow State University, Moscow, Russia

[102] Fakultät für Physik, Ludwig-Maximilians-Universität München, Munich, Germany

[103] Max-Planck-Institut für Physik (Werner-Heisenberg-Institut), Munich, Germany

[104] Nagasaki Institute of Applied Science, Nagasaki, Japan

[105] Graduate School of Science and Kobayashi-Maskawa Institute, Nagoya University, Nagoya, Japan

[106] [a]INFN Sezione di Napoli, Naples, Italy; [b]Dipartimento di Fisica, Università di Napoli, Naples, Italy

[107] Department of Physics and Astronomy, University of New Mexico, Albuquerque, NM, USA

[108] Institute for Mathematics, Astrophysics and Particle Physics, Radboud University Nijmegen/Nikhef, Nijmegen, Netherlands

[109] Nikhef National Institute for Subatomic Physics and University of Amsterdam, Amsterdam, Netherlands

[110] Department of Physics, Northern Illinois University, DeKalb, IL, USA

[111] Budker Institute of Nuclear Physics, SB RAS, Novosibirsk, Russia

[112] Department of Physics, New York University, New York, NY, USA

[113] Ohio State University, Columbus, OH, USA

[114] Faculty of Science, Okayama University, Okayama, Japan

[115] Homer L. Dodge Department of Physics and Astronomy, University of Oklahoma, Norman, OK, USA

[116] Department of Physics, Oklahoma State University, Stillwater, OK, USA

[117] Palacký University, RCPTM, Olomouc, Czech Republic

[118] Center for High Energy Physics, University of Oregon, Eugene, OR, USA

[119] LAL, Univ. Paris-Sud, CNRS/IN2P3, Université Paris-Saclay, Orsay, France

[120] Graduate School of Science, Osaka University, Osaka, Japan

[121] Department of Physics, University of Oslo, Oslo, Norway

[122] Department of Physics, Oxford University, Oxford, UK

[123] [a]INFN Sezione di Pavia, Pavia, Italy; [b]Dipartimento di Fisica, Università di Pavia, Pavia, Italy

[124] Department of Physics, University of Pennsylvania, Philadelphia, PA, USA

[125] National Research Centre "Kurchatov Institute" B.P. Konstantinov Petersburg Nuclear Physics Institute, St. Petersburg, Russia

[126] [a]INFN Sezione di Pisa, Pisa, Italy; [b]Dipartimento di Fisica E. Fermi, Università di Pisa, Pisa, Italy

[127] Department of Physics and Astronomy, University of Pittsburgh, Pittsburgh, PA, USA

[128] [a]Laboratório de Instrumentação e Física Experimental de Partículas-LIP, Lisbon, Portugal; [b]Faculdade de Ciências, Universidade de Lisboa, Lisbon, Portugal; [c]Department of Physics, University of Coimbra, Coimbra, Portugal; [d]Centro de Física Nuclear da Universidade de Lisboa, Lisbon, Portugal; [e]Departamento de Fisica, Universidade do Minho, Braga, Portugal; [f]Departamento de Fisica Teorica y del Cosmos and CAFPE, Universidad de Granada, Granada, Spain; [g]Dep Fisica and CEFITEC of Faculdade de Ciencias e Tecnologia, Universidade Nova de Lisboa, Caparica, Portugal

[129] Institute of Physics, Academy of Sciences of the Czech Republic, Prague, Czech Republic

[130] Czech Technical University in Prague, Prague, Czech Republic

[131] Faculty of Mathematics and Physics, Charles University in Prague, Prague, Czech Republic

[132] State Research Center Institute for High Energy Physics (Protvino), NRC KI, Protvino, Russia

[133] Particle Physics Department, Rutherford Appleton Laboratory, Didcot, UK

[134] [a] INFN Sezione di Roma, Rome, Italy; [b] Dipartimento di Fisica, Sapienza Università di Roma, Rome, Italy

[135] [a] INFN Sezione di Roma Tor Vergata, Rome, Italy; [b] Dipartimento di Fisica, Università di Roma Tor Vergata, Rome, Italy

[136] [a] INFN Sezione di Roma Tre, Rome, Italy; [b] Dipartimento di Matematica e Fisica, Università Roma Tre, Rome, Italy

[137] [a] Faculté des Sciences Ain Chock, Réseau Universitaire de Physique des Hautes Energies-Université Hassan II, Casablanca, Morocco; [b] Centre National de l'Energie des Sciences Techniques Nucleaires, Rabat, Morocco; [c] Faculté des Sciences Semlalia, Université Cadi Ayyad, LPHEA-Marrakech, Marrakech, Morocco; [d] Faculté des Sciences, Université Mohamed Premier and LPTPM, Oujda, Morocco; [e] Faculté des Sciences, Université Mohammed V, Rabat, Morocco

[138] DSM/IRFU (Institut de Recherches sur les Lois Fondamentales de l'Univers), CEA Saclay (Commissariat à l'Energie Atomique et aux Energies Alternatives), Gif-sur-Yvette, France

[139] Santa Cruz Institute for Particle Physics, University of California Santa Cruz, Santa Cruz, CA, USA

[140] Department of Physics, University of Washington, Seattle, WA, USA

[141] Department of Physics and Astronomy, University of Sheffield, Sheffield, UK

[142] Department of Physics, Shinshu University, Nagano, Japan

[143] Fachbereich Physik, Universität Siegen, Siegen, Germany

[144] Department of Physics, Simon Fraser University, Burnaby, BC, Canada

[145] SLAC National Accelerator Laboratory, Stanford, CA, USA

[146] [a] Faculty of Mathematics, Physics and Informatics, Comenius University, Bratislava, Slovak Republic; [b] Department of Subnuclear Physics, Institute of Experimental Physics of the Slovak Academy of Sciences, Kosice, Slovak Republic

[147] [a] Department of Physics, University of Cape Town, Cape Town, South Africa; [b] Department of Physics, University of Johannesburg, Johannesburg, South Africa; [c] School of Physics, University of the Witwatersrand, Johannesburg, South Africa

[148] [a] Department of Physics, Stockholm University, Stockholm, Sweden; [b] The Oskar Klein Centre, Stockholm, Sweden

[149] Physics Department, Royal Institute of Technology, Stockholm, Sweden

[150] Departments of Physics and Astronomy and Chemistry, Stony Brook University, Stony Brook, NY, USA

[151] Department of Physics and Astronomy, University of Sussex, Brighton, UK

[152] School of Physics, University of Sydney, Sydney, Australia

[153] Institute of Physics, Academia Sinica, Taipei, Taiwan

[154] Department of Physics, Technion: Israel Institute of Technology, Haifa, Israel

[155] Raymond and Beverly Sackler School of Physics and Astronomy, Tel Aviv University, Tel Aviv, Israel

[156] Department of Physics, Aristotle University of Thessaloniki, Thessaloniki, Greece

[157] International Center for Elementary Particle Physics and Department of Physics, The University of Tokyo, Tokyo, Japan

[158] Graduate School of Science and Technology, Tokyo Metropolitan University, Tokyo, Japan

[159] Department of Physics, Tokyo Institute of Technology, Tokyo, Japan

[160] Tomsk State University, Tomsk, Russia

[161] Department of Physics, University of Toronto, Toronto, ON, Canada

[162] [a] INFN-TIFPA, Trento, Italy; [b] University of Trento, Trento, Italy

[163] [a] TRIUMF, Vancouver, BC, Canada; [b] Department of Physics and Astronomy, York University, Toronto, ON, Canada

[164] Faculty of Pure and Applied Sciences, and Center for Integrated Research in Fundamental Science and Engineering, University of Tsukuba, Tsukuba, Japan

[165] Department of Physics and Astronomy, Tufts University, Medford, MA, USA

[166] Department of Physics and Astronomy, University of California Irvine, Irvine, CA, USA

[167] [a] INFN Gruppo Collegato di Udine, Sezione di Trieste, Udine, Italy; [b] ICTP, Trieste, Italy; [c] Dipartimento di Chimica, Fisica e Ambiente, Università di Udine, Udine, Italy

[168] Department of Physics and Astronomy, University of Uppsala, Uppsala, Sweden

[169] Department of Physics, University of Illinois, Urbana, IL, USA

[170] Instituto de Fisica Corpuscular (IFIC) and Departamento de Fisica Atomica, Molecular y Nuclear and Departamento de Ingeniería Electrónica and Instituto de Microelectrónica de Barcelona (IMB-CNM), University of Valencia and CSIC, Valencia, Spain

[171] Department of Physics, University of British Columbia, Vancouver, BC, Canada

[172] Department of Physics and Astronomy, University of Victoria, Victoria, BC, Canada

[173] Department of Physics, University of Warwick, Coventry, UK

[174] Waseda University, Tokyo, Japan

[175] Department of Particle Physics, The Weizmann Institute of Science, Rehovot, Israel

[176] Department of Physics, University of Wisconsin, Madison, WI, USA

[177] Fakultät für Physik und Astronomie, Julius-Maximilians-Universität, Würzburg, Germany

[178] Fakultät für Mathematik und Naturwissenschaften, Fachgruppe Physik, Bergische Universität Wuppertal, Wuppertal, Germany

[179] Department of Physics, Yale University, New Haven, CT, USA

[180] Yerevan Physics Institute, Yerevan, Armenia

[181] Centre de Calcul de l'Institut National de Physique Nucléaire et de Physique des Particules (IN2P3), Villeurbanne, France

[a] Also at Department of Physics, King's College London, London, UK

[b] Also at Institute of Physics, Azerbaijan Academy of Sciences, Baku, Azerbaijan

[c] Also at Novosibirsk State University, Novosibirsk, Russia

[d] Also at TRIUMF, Vancouver, BC, Canada

[e] Also at Department of Physics and Astronomy, University of Louisville, Louisville, KY, USA

[f] Also at Physics Department, An-Najah National University, Nablus, Palestine

[g] Also at Department of Physics, California State University, Fresno, CA, USA

[h] Also at Department of Physics, University of Fribourg, Fribourg, Switzerland

[i] Also at Departament de Fisica de la Universitat Autonoma de Barcelona, Barcelona, Spain

[j] Also at Departamento de Fisica e Astronomia, Faculdade de Ciencias, Universidade do Porto, Porto, Portugal

[k] Also at Tomsk State University, Tomsk, Russia

[l] Also at Universita di Napoli Parthenope, Napoli, Italy

[m] Also at Institute of Particle Physics (IPP), Canada

[n] Also at National Institute of Physics and Nuclear Engineering, Bucharest, Romania

[o] Also at Department of Physics, St. Petersburg State Polytechnical University, St. Petersburg, Russia

[p] Also at Department of Physics, The University of Michigan, Ann Arbor, MI, USA

[q] Also at Centre for High Performance Computing, CSIR Campus, Rosebank, Cape Town, South Africa

[r] Also at Louisiana Tech University, Ruston, LA, USA

[s] Also at Institucio Catalana de Recerca i Estudis Avancats, ICREA, Barcelona, Spain

[t] Also at Graduate School of Science, Osaka University, Osaka, Japan

[u] Also at Institute for Mathematics, Astrophysics and Particle Physics, Radboud University Nijmegen/Nikhef, Nijmegen, Netherlands

[v] Also at Department of Physics, The University of Texas at Austin, Austin, TX, USA

[w] Also at Institute of Theoretical Physics, Ilia State University, Tbilisi, Georgia

[x] Also at CERN, Geneva, Switzerland

[y] Also at Georgian Technical University (GTU), Tbilisi, Georgia

[z] Also at Ochadai Academic Production, Ochanomizu University, Tokyo, Japan

[aa] Also at Manhattan College, New York, NY, USA

[ab] Also at Academia Sinica Grid Computing, Institute of Physics, Academia Sinica, Taipei, Taiwan

[ac] Also at School of Physics, Shandong University, Shandong, China

[ad] Also at Department of Physics, California State University, Sacramento CA, USA

[ae] Also at Moscow Institute of Physics and Technology, State University, Dolgoprudny, Russia

[af] Also at Departement de Physique Nucleaire et Corpusculaire, Université de Genève, Geneva, Switzerland

[ag] Also at Eotvos Lorand University, Budapest, Hungary

[ah] Also at International School for Advanced Studies (SISSA), Trieste, Italy

[ai] Also at Department of Physics and Astronomy, University of South Carolina, Columbia, SC, USA

[aj] Also at Institut de Física d'Altes Energies (IFAE), The Barcelona Institute of Science and Technology, Barcelona, Spain

[ak] Also at School of Physics and Engineering, Sun Yat-sen University, Guangzhou, China

[al] Also at Institute for Nuclear Research and Nuclear Energy (INRNE) of the Bulgarian Academy of Sciences, Sofia, Bulgaria

am Also at Faculty of Physics, M.V.Lomonosov Moscow State University, Moscow, Russia

an Also at Institute of Physics, Academia Sinica, Taipei, Taiwan

ao Also at National Research Nuclear University MEPhI, Moscow, Russia

ap Also at Department of Physics, Stanford University, Stanford, CA, USA

aq Also at Institute for Particle and Nuclear Physics, Wigner Research Centre for Physics, Budapest, Hungary

ar Also at Giresun University, Faculty of Engineering, Turkey

as Also at Flensburg University of Applied Sciences, Flensburg, Germany

at Also at University of Malaya, Department of Physics, Kuala Lumpur, Malaysia

au Also at CPPM, Aix-Marseille Université and CNRS/IN2P3, Marseille, France

* Deceased